Physics – Uspekhi **58** (9) 906 – 924 (2015)

FROM THE "USPEKHI FIZICHESKIKH NAUK" ARCHIVE

PACS numbers: **01.65.+g**, **05.40.–a**, **34.35.+a**

100th ANNIVERSARY OF THE BIRTH OF E M LIFSHITZ

Molecular attraction of condensed bodies*

B V Derjaguin, I I Abrikosova, E M Lifshitz

DOI: 10.3367/UFNe.0185.201509i.0981

Contents

Abstract. From the Editorial Board. As a contribution to commemorating the 100th anniversary of the birth of Evgenii Mikhailovich Lifshitz, it was found appropriate by the Editorial Board of *Uspekhi Fizicheskikh Nauk* (*UFN*) [*Physics – Uspekhi*] journal that the materials of the jubilee-associated Scientific Session of the Physical Sciences Division of the Russian Academy of Sciences published in this issue (pp. 877 – 905) be augmented by the review paper "Molecular attraction of condensed bodies" reproduced from a 1958 *UFN* issue. Included in this review, in addition to an *ad hoc* account by Evgenii Mikhailovich Lifshitz of his theory of molecular attractive forces between condensed bodies (first published in *Zhurnal Eksperimental'noi i Teoreticheskoi Fiziki* (*ZhETF*) in 1955 and in its English translation *Journal of Experimental and Theoretical Physics* (*JETP*) in 1956), is a summary of a series of experimental studies beginning in 1949 by Irina Igorevna Abrikosova at the Institute of Physical Chemistry of the Academy of Sciences of the USSR in a laboratory led by Boris Vladimirovich Derjaguin (1902–1994), a Corresponding Member of the USSR Academy of Sciences. In 1958, however, *UFN* was not yet available in English translation, so the material of the review is insufficiently accessible to the present-day English-speaking reader. This is the reason why the *UFN* Editorial Board decided to contribute to celebrating the 100th anniversary of E M Lifshitz's birthday by reproducing on the journal's pages a 1958 review paper which contains both E M Lifshitz's theory itself and the experimental data that underpinned it (for an account of how Evgenii Mikhailovich Lifshitz was enlisted to explain the experimental results of I I Abrikosova and B V Derjaguin, see the letter to the editors by N P Danilova on page 925 of this jubilee collection of publications).

Keywords: molecular attraction, molecular forces, long-range forces, fluctuation forces, dispersion interactions

1. Introduction

Besides the familiar valence forces capable of saturation and having a comparatively short radius of action (several angströms), there are forces of attraction acting between any two atoms or molecules, unable to be saturated and decreasing much more slowly with distance. These molecular forces form the basis of a wide field of fundamental problems in physical chemistry and molecular physics. Surface tension, capillarity, physical adsorption, and many other surface phenomena are explained first and foremost by molecular forces; they determine not only most of the properties of molecular crystals and liquids but also the phenomena of vapor condensation and gas liquefaction.

The attractive forces between atoms and molecules naturally give rise to analogous 'molecular attraction' between two macroscopic bodies whose surfaces have been brought within a short distance of one another. As an example of their action, we can see coagulation processes in colloidal and aerosol systems caused by the intermolecular interaction between two colloidal particles when they approach each other. The idea of the role of molecular forces

* Sections 1, 2, 4, and 5 written by B V Derjaguin and I I Abrikosova; Section 3 written by E M Lifshitz.

This paper, originally published in the journal *Uspekhi Fizicheskikh Nauk* (*UFN*) Vol. 64, No. 3, pp. 493 – 528 (1958) is here reissued in accordance with *UFN*'s present-day style standards.

First published in *Uspekhi Fizicheskikh Nauk* **64** (3) 493 – 528 (1958)
Uspekhi Fizicheskikh Nauk **185** (9) 981 – 1001 (2015)
DOI: 10.3367/UFNr.0185.201509i.0981
Translated by Yu V Morozov; edited by A Radzig

was first put forward in a short note by Kallmann and Willstätter [1]. These forces formed the basis for a quantitative theory of stability and coagulation of colloids [2–9] along with taking account of the repulsive forces between diffuse double ionic layers of approaching particles. Some authors, as, for instance, Langmuir [10], believed, however, that the theory of colloidal systems could be constructed without assuming the existence of interactions caused by the van der Waals attractive forces between molecules of neighboring colloidal particles. They have cast doubt on the existence of similar forces in themselves over distances significantly exceeding those among neighboring molecules. Thus, the questions of the magnitude of the force or the energy of molecular interactions between macroscopic particles and their dependence on the distance between them are some of the basic problems in the theory of stability and coagulation of colloids. The same forces must play an important role in other colloidal processes, such as thixotropy, and the formation of tactoids and coacervates.

Despite the considerable theoretical and applied significance of molecular forces, investigations into their nature and the development of the relevant theory have a rather short history. P Lebedew [11, 12] and B B Golitzin [13] were among the first to formulate the correct view on the nature of molecular forces.

In 1894, P Lebedew [11, 12] considered the ponderomotive action of waves on resonators and arrived at the following conclusion: "Interpretation of light vibrations by Hertz as electromagnetic processes conceals one more, thus far untouched, problem that of radiation sources and processes proceeding in a molecular vibrator when it gives up light energy to the surrounding space. This problem leads, on the one hand, to *spectroscopic analysis* and, on the other hand, quite unexpectedly, to one of the most complicated problems of modern physics, i.e., the theory of *molecular forces*. The latter ensues from the following considerations: from the standpoint of the electromagnetic theory of light, we have to recognize the existence of *ponderomotive forces* between two light-emitting molecules as between two vibrators in which electromagnetic vibrations are excited; these forces arise from electrodynamic interactions between variable electric currents flowing in molecules (in accordance with Ampere's laws) or between variable charges in them (in accordance with the Coulomb laws). Therefore, we must assert that in this case *molecular forces* exist between molecules closely linked to radiative processes..."

"...The most interesting and difficult to interpret is the case of a physical body in which many molecules simultaneously act on one another and whose vibrations are not independent owing to their close proximity. If this problem can some day be fully resolved, results of spectroscopic analysis will be used to predict by calculation the forces between molecules due to their mutual emission of radiation, elucidate their temperature dependences, compare theoretical and experimental findings, and thereby solve a key problem of molecular physics: whether all the so-called 'molecular forces' reduce to the aforementioned ponderomotive action of light emission, i.e., to electromagnetic forces, or whether they also involve other forces of a yet unknown nature."

However, the first quantitative theories of molecular forces could be established only after the structure of atoms and molecules had been elucidated. The concept of molecular dipoles provided a basis for the Debye theory of orientation forces and the Keesom theory of inductive forces. But the interaction between nondipole molecules remained obscure, especially between noble gas molecules having a spherically symmetric electron shell. Only the application of quantum mechanics enabled London [14] to explain the existence of these forces and develop, in the first approximation, a general quantitative theory of molecular forces. This general theory refined, among other things, the classical formulas for polar molecule interaction.

For the case of large distances between molecules relative to their diameter (i.e., mostly for gases), the theory leads to interaction forces decreasing inversely proportional to the seventh power of the intermolecular distance. In solids, however, where the rotation of molecules is not free, there can be forces that decrease much more slowly with distance. At the same time, at small intermolecular distances characteristic of condensed bodies, forces decreasing more rapidly with distance, e.g., those due to quadrupole moments, may acquire significance. Therefore, it is understandable why the previous attempts at a quantitative verification of the theory of molecular forces could not, in principle, (and did not) yield reasonably accurate and convincing results. Indeed, all these attempts were based on the comparison with a theory of integrated effects in which those factors prevail that depend on the interaction of molecules spaced apart by distances commensurate with their radii.

This inference holds, for example, for the methods of a theory verification based on determination of constant a in the van der Waals equation, sublimation and evaporation heat, energies of adsorption and wetting. In all these cases, an exact comparison with the theory encounters difficulties, because any theory of molecular forces is, strictly speaking, inapplicable at such short distances. Moreover, the result depends on the combination of forces of various types (e.g., quadrupole ones) that, in addition, depend on frequently unknown orientations of molecules and the asymmetry of their force fields.

Much more rigorous verification of the existing theories of molecular forces is possible based on the results of experimental studies of effects depending only on the action of molecular forces at distances larger than molecular diameters. From this standpoint, it is of special interest to measure the molecular attraction between two solid bodies separated by a gap as wide as many molecular diameters, i.e., as in Cavendish's experiments on gravitational forces and in Coulomb's experiments on the forces acting between electrical charges. Such experiments, unlike measurements of adhesion forces at contact [15], make it possible to verify theories of intermolecular interaction (supplemented, of course, by one method or another of their summation for the molecules that form the macroscopic bodies of interest) at distances at which only forces of the same nature remain and the limitations on the validity of the theories do not apply.

As far as we know, no experiments of this kind, even if of a qualitative character, were reported as of 1951, the cause certainly being obvious experimental difficulties, discussed below. Therefore, we describe here the method for direct measurement of molecular attraction between two solid bodies as a function of the width of the gap separating them. The method was developed in the Laboratory of Surface Phenomena, Institute of Physical Chemistry, USSR Academy of Sciences, in 1951. Special emphasis is laid on the application of the data obtained to the verification of the relevant theories and to certain problems of colloid chemistry

and the physics of surface phenomena. To begin with, we consider the problem of molecular forces for microscopic objects and undertake a critical analysis of the commonly applied methods for the summation of these forces to derive forces of interaction between macroscopic objects.

In contrast to these nonrigorous methods, the new approach to the interaction of macroscopic objects proposed by one of the authors (E M L) has not only led to the first wholly general and rigorous theory of the molecular interaction of macroscopic objects with both macroscopic and microscopic objects, but also provided a simpler justification for the law of interaction between microscopic objects — that is, individual pairs of molecules. Lifshitz's theory is presented in Section 3.

2. Theory of molecular interaction between microscopic objects and criticism of its application to macroscopic objects

2.1 Microscopic objects

According to London [14], the interaction energy u between individual atoms or molecules at distances r longer than their dimensions is given by

$$u = -\frac{C}{r^6}\,, \tag{1}$$

where C is always a positive constant for a given type of atoms calculated from the matrix elements of electric moments of both atoms. London [16] emphasizes the possibility of using the approximate formula

$$u = -\frac{3}{4}\frac{h\nu_0\alpha^2}{r^6} \tag{2}$$

for many simple molecules, where $h\nu_0$ is the characteristic energy term that can be derived from the experimentally found formula for optical dispersion of a given gas, and α is the molecular polarizability. Clearly, the intermolecular attractive forces $F = -\,\mathrm{d}u/\mathrm{d}r$ change inversely proportional to the seventh power of the distance between the molecules.

London's theory has limits of applicability; namely, the calculation becomes invalid not only for very small interatomic distances (when their own wave functions overlap) but also for large enough distances (when the effect of electromagnetic retardation needs to be considered).

The electromagnetic retardation was taken into account by Casimir and Polder [17], who resorted to quantum electrodynamics. They applied the same perturbation method, but their perturbation operator contained, along with London's electrostatic attractive force, the interaction of the radiation field of one atom with another atom and vice versa.

According to the Casimir–Polder theory, in the limit of $r \gg \lambda_i$ (where λ_i is all the absorption or emission wavelengths of a given atom), the energy of interaction between two atoms with static polarizability α is given by

$$u = -\frac{23}{4\pi}\frac{\hbar c\alpha^2}{r^7}\,, \tag{3}$$

or

$$u = -\frac{C_1}{r^7}\,, \quad \text{where} \quad C_1 = 251e^2\alpha^2\,.$$

Here, $\hbar$, c, and e have their usual meanings.

The force of attraction between two atoms in this limiting case varies with distance as r^{-8}.

Thus, current theories explain the origin of intermolecular attraction and permit calculating the interaction of free atoms and molecules. The most detailed discussion of this issue can be found in the reviews by London [18] and Margenau [19].

2.2 Macroscopic objects

Molecular attraction between objects consisting of a large number of molecules is usually seen, on the assumption of the additivity of the London forces acting in between objects, as the sum of attractive forces between all pairs of molecules making up a given body. For example, de Boer [20] and Hamaker [21] found the interaction between two bodies containing q molecules per unit volume by integrating elementary interactions obeying the London law. Hamaker derived the formulas for the energy and attractive force between two bodies shaped like a sphere, a sphere and an infinite flat wall, and finally two such infinite flat parallel walls. If the shortest distance between the surfaces is much smaller than their radius of curvature R, the interaction energy in the first case is given by the expression

$$U = -\frac{AR}{12H}\,, \tag{4}$$

and the attractive force by

$$F = \frac{AR}{12H^2}\,; \tag{4'}$$

in the second case, the energy equals

$$U = -\frac{AR}{6H}\,, \tag{5}$$

and the force

$$F = \frac{AR}{6H^2}\,; \tag{5'}$$

finally, the energy per unit area for two infinite plates is written out as

$$u = -\frac{A}{12\pi H^2} \tag{6}$$

and the force per unit area

$$f = \frac{A}{6\pi H^3}\,; \tag{6'}$$

here, H is the shortest distance between the bodies, and A is the constant introduced by Hamaker that depends on the nature of the bodies and equals the product $\pi^2 q^2 C$. These formulas are usually used to calculate the interaction force between colloidal particles and other macroscopic objects (Hamaker–London interaction).

Analogous calculations taking account of the electromagnetic retardation effect yield, in the limiting case of large enough distances, the expression

$$u = -\frac{A_1}{30\pi H^3} \tag{7}$$

for the energy per unit area of the parallel plates, and for the force acting on unit area the formula

$$f = \frac{A_1}{10\pi H^4}\,, \tag{7'}$$

where A_1 is the product $\pi^2 q^2 C_1$.

Strictly speaking, the additivity of London forces for condensed bodies has neither theoretical nor experimental substantiation: they would be possible only in the unrealizable case of two strongly rarefied bodies (i.e., gases) separated by a gap. Moreover, atomic and molecular characteristics, e.g., α and $h\nu_0$, are altered in condensed systems compared with the properties of isolated atoms and molecules due to the mutual influence of neighboring particles. For this reason, the contribution to the molecular interaction from individual molecules depends on their coordination and concentration; for surface molecules, it depends on the number of neighbors. Assuming strict additivity, one has to take, for consistency, the values of α and $h\nu_0$ for isolated molecules, which would certainly involve an error. Otherwise, it is difficult to obtain 'true' values of α and $h\nu_0$, because they are not easy to determine and are often totally unknown for condensed systems.

Apart from the absence of physical rigor in such an approach, it is opportune to note that the calculation of constants A and A_1 is always very difficult in practice, even for isolated atoms and molecules. In most cases, it is impossible to obtain quantitative data because the values of α and $h\nu_0$ remain unknown for many atoms. The only way out in such cases is to determine the polarizability from solid body refraction and thereby substitute condensed medium characteristics into the London formulas holding for the interaction between individual atoms.

Besides difficulties encountered in finding the parameters of the formula for A, the strict applicability of the approximate formula (2) is also doubtful, the validity of which having been proved by London only for certain simple molecules.

3. Theory of molecular attractive forces between condensed bodies

As mentioned in the Introduction, the calculation of molecular attractive forces acting between condensed bodies is impossible based on the known interaction between individual molecules. It would be legitimate only for sufficiently rarefied bodies, such as gases, i.e., in the obviously unrealizable case.

However, this issue can be addressed, in contrast to such a 'microscopic' approach, from a quite different, purely macroscopic, point of view by considering the interacting bodies as continuous media. The legitimacy of such an approach ensues from the assumption that the distance between body surfaces is greater than interatomic distances no matter how small it actually is.

The principal idea behind the theory is that the interaction of the bodies is mediated through a fluctuating electromagnetic field. Due to thermodynamic fluctuations, such a field is always present in the interior of any material medium and also extends beyond its boundaries. A well-known manifestation of this field is thermal radiation from a body, even though it does not represent the entire fluctuation field outside the body. It is obvious even from the fact that electromagnetic fluctuations occur even at absolute zero when there is no thermal radiation; at this temperature, the fluctuations are of a purely quantum character and associated with so-called zero-point vibrations of the electromagnetic field.

Let us imagine that both bodies are semiinfinite regions separated from each other by a gap of a given width l with plane-parallel boundaries. The aim of the calculations is to define the fluctuating electromagnetic field in such a system, in particular, in the gap volume. Then, the force f acting on either surface (on 1 cm^2 of each) can be determined as the mean value of the respective component of the Maxwell stress tensor.[1]

It should be emphasized that such an approach to the problem is characterized by full generality and is applicable to any bodies at any temperatures, whatever their molecular nature (ionic or molecular crystals, amorphous bodies, metals, dielectrics, etc.). An important feature of the method attributable to the involvement of exact Maxwell equations is that it automatically takes into account retardation effects related to the finite propagation velocity of electromagnetic interactions. These effects become essential if the distance l be large enough: $l \gg \lambda_0$, where λ_0 are the characteristic wavelengths for the absorption spectra of these bodies.

The general method for calculating electromagnetic fluctuations was developed by S M Rytov; its detailed exposition was presented in his book [22] (see also monograph [23, Chapter XIII]). Neither the detailed characteristics of the method nor the cumbersome calculations it implies are presented here (those interested in this issue are addressed to original paper [24]). Only the final results of the calculations will be cited.

The formulas below contain function $\varepsilon(\omega)$, i.e., the dielectric constant of the body as a function of the electromagnetic field frequency.[2] To recall, $\varepsilon(\omega)$ is, generally speaking, a complex quantity $[\varepsilon = \varepsilon'(\omega) + \mathrm{i}\varepsilon''(\omega)]$, with its imaginary part always being positive and determining the energy dissipation of an electromagnetic wave propagating along the body. The function $\varepsilon(\omega)$ is related to the refractive index n and the absorption coefficient $\varkappa$ of the medium by the familiar expression $\sqrt{\varepsilon} = n + \mathrm{i}\varkappa$. Also, the formal consideration of $\varepsilon(\omega)$ as a function of complex variable ω allows us to establish certain integral relationships between $\varepsilon'(\omega)$ and $\varepsilon''(\omega)$ — the so-called Kramers–Kronig formulas (see, for instance, monograph [23, § 62]). One of the consequences of these formulas is the relation

$$\varepsilon(\mathrm{i}\xi) = 1 + \frac{2}{\pi}\int_0^\infty \frac{\omega\varepsilon''(\omega)}{\omega^2 + \xi^2}\,\mathrm{d}\omega \tag{8}$$

defining the values of function ε of a purely imaginary argument from those of function $\varepsilon''(\omega)$ of real arguments ω; $\varepsilon(\mathrm{i}\xi)$ is a real quantity decreasing monotonically from ε_0 (electrostatic permittivity) at $\xi = 0$ to 1 as $\xi \to \infty$.

The influence of temperature on the attractive force acting between bodies is usually unessential (see below) and can be regarded as unessential. In this case, the final theoretical formula for the attractive force has the form

$$f = \frac{\hbar}{2\pi^3 c^3}\int_0^\infty\int_1^\infty \left\{\left[\frac{(s_1+p)(s_2+p)}{(s_1-p)(s_2-p)}\exp\left(\frac{2p\xi l}{c}\right) - 1\right]^{-1} + \left[\frac{(s_1+\varepsilon_1 p)(s_2+\varepsilon_2 p)}{(s_1-\varepsilon_1 p)(s_2-\varepsilon_2 p)}\exp\left(\frac{2p\xi l}{c}\right) - 1\right]^{-1}\right\} p^2\xi^3\,\mathrm{d}p\,\mathrm{d}\xi\,, \tag{9}$$

[1] The stress averaged over time vanishes in the fluctuation field, whereas mean values of quadratic expressions, including Maxwell's stresses, remain nonzero.

[2] We suggest that the permeability of a body can be taken equal to unity as is usually the case (see below).

where ε denotes $\varepsilon(\mathrm{i}\xi)$, subscripts 1 and 2 refer to the two bodies of interest, and the following notation was introduced:

$$s = \sqrt{\varepsilon(\mathrm{i}\xi) - 1 + p^2}\,.$$

It then follows that the attractive force can be calculated, in principle, for any distance l if functions $\varepsilon_1(\mathrm{i}\xi)$, $\varepsilon_2(\mathrm{i}\xi)$ are known for both bodies. However, $\varepsilon(\mathrm{i}\xi)$ can be determined, in accordance with formula (9), from the known (in a wide enough spectral range) function $\varepsilon''(\omega)$. In other words, the imaginary part $\varepsilon''(\omega)$ of permittivity is the sole characteristic of the macroscopic properties of bodies that determines the force of molecular attraction between them.

The complicated general formula (9) is significantly simplified in two important limiting cases.

Let us consider first the case of 'short separations', $l \ll \lambda_0$. Due to the presence of an exponentially growing factor $\exp(2p\xi l/c)$ in the denominators of the integrand in Eqn (9), the main role in integration over $\mathrm{d}p$ is played by such p values that $p\xi l/c \approx 1$. In this case $p \gg 1$, which allows assuming, with sufficient accuracy, that $s_1 \approx s_2 \approx p$. In this approximation, the first term in the braces in formula (9) vanishes. The second term, after the introduction of variable $x = 2pl\xi/c$, yields

$$f = \frac{\hbar}{16\pi^2 l^3} \times \int_0^\infty \int_0^\infty \frac{x^2\,\mathrm{d}x\,\mathrm{d}\xi}{[(\varepsilon_1+1)/(\varepsilon_1-1)][(\varepsilon_2+1)/(\varepsilon_2-1)]^2 \exp x - 1} \qquad (10)$$

(in this approximation, the lower limit of integration over $\mathrm{d}x$ is replaced by zero). This formula can be further simplified, with a practically sufficient accuracy, by neglecting unity in the denominator of the integrand. Then, integration over $\mathrm{d}x$ is an elementary procedure and one arrives at

$$f = \frac{\hbar}{8\pi^2 l^3} \int_0^\infty \frac{\big(\varepsilon_1(\mathrm{i}\xi) - 1\big)\big(\varepsilon_2(\mathrm{i}\xi) - 1\big)}{\big(\varepsilon_1(\mathrm{i}\xi) + 1\big)\big(\varepsilon_2(\mathrm{i}\xi) + 1\big)}\,\mathrm{d}\xi\,. \qquad (11)$$

Thus, the attractive force for $l \ll \lambda_0$ is inversely proportional to the cube of the body spacing with a coefficient that can be calculated using the known functions $\varepsilon_1(\mathrm{i}\xi)$, $\varepsilon_2(\mathrm{i}\xi)$.[3]

We can demonstrate how the passage to the limit of interaction between individual atoms is carried out in the written formulas. To this end, we assume in a formal mode that both media are sufficiently rarefied. From the standpoint of macroscopic electrodynamics, this means that their permittivities are close to unity, i.e., the differences $\varepsilon_1 - 1$ and $\varepsilon_2 - 1$ are small. Then, it follows from formula (10) or (11) that

$$f = \frac{\hbar}{32\pi^2 l^3} \int_0^\infty \big(\varepsilon_1(\mathrm{i}\xi) - 1\big)\big(\varepsilon_2(\mathrm{i}\xi) - 1\big)\,\mathrm{d}\xi\,.$$

Expressing $\varepsilon(\mathrm{i}\xi)$ in terms of the values of $\varepsilon''(\omega)$ at real frequencies ω, in accordance with relation (8), we obtain

$$f = \frac{\hbar}{8\pi^4 l^3} \int_0^\infty \int_0^\infty \int_0^\infty \frac{\omega_1\omega_2\varepsilon_1''(\omega_1)\,\varepsilon_2''(\omega_2)}{(\omega_1^2 + \xi^2)(\omega_2^2 + \xi^2)}\,\mathrm{d}\xi\,\mathrm{d}\omega_1\,\mathrm{d}\omega_2\,.$$

[3] As mentioned above, the differences $\varepsilon(\mathrm{i}\xi) - 1$ decrease monotonically and tend to zero as ξ increases. Simultaneously, the integrand in formula (10) decreases and the values of ξ, after a certain ξ_0, cease to make a substantial contribution to the integral; the smallness condition for l means, strictly speaking, that $l \ll c/\xi_0$.

The integration over $\mathrm{d}\xi$ is an elementary operation yielding

$$f = \frac{\hbar}{16\pi^3 l^3} \int_0^\infty \int_0^\infty \frac{\varepsilon_1''(\omega_1)\,\varepsilon_2''(\omega_2)}{\omega_1 + \omega_2}\,\mathrm{d}\omega_1\,\mathrm{d}\omega_2\,. \qquad (12)$$

This force, considered as a result of the interaction between individual pairs of molecules (one in each of the two bodies), corresponds to an interaction with potential energy

$$u(r) = -\frac{3\hbar}{8\pi^4 r^6 N^2} \int_0^\infty \int_0^\infty \frac{\varepsilon_1''(\omega_1)\,\varepsilon_2''(\omega_2)}{\omega_1 + \omega_2}\,\mathrm{d}\omega_1\,\mathrm{d}\omega_2\,, \qquad (13)$$

where r is the distance between the molecules, and N is the number of molecules per unit volume of the body.[4] In order to bring this expression to the familiar form, one should bear in mind that the imaginary part $\varepsilon''(\omega)$ of the dielectric constant of a gas is related to the spectral density $\varphi(\omega)$ of 'oscillator strengths' known from spectroscopy through the expression

$$\omega\varepsilon''(\omega) = \frac{2\pi^2 e^2}{m} N\varphi(\omega)\,.$$

Suppose, for instance, that we are considering the interaction of two hydrogen atoms. Taking advantage of the known expression

$$\varphi_{0n} = \frac{2m}{\hbar^2}(E_n - E_0)|X_{0n}|^2$$

for the oscillator strength of the transition between the states E_n and E_0 (with X_{0n} being the corresponding matrix element of the electron coordinate in an atom) and changing in formula (13) from integration over frequencies to summation over atomic energy levels, we find

$$u(r) = -\frac{6}{r^6} \sum_{n,m} \frac{|X_{0n}|^2 |X_{0m}|^2}{(E_n - E_0) + (E_m - E_0)}\,,$$

which agrees exactly with London's known quantum-mechanical formula [14] for van der Waals forces (neglecting retardation effects). Thus, this 'microscopic' formula can be derived from a purely macroscopic theory.

We now move to the opposite case of 'large separations' that are greater than the fundamental wavelengths ($l \gg \lambda_0$) in the absorption spectrum of bodies.

Let us again introduce a new integration variable $x = 2pl\xi/c$ in general formula (9) but keep as the second variable not ξ but rather p:

$$f = \frac{\hbar c}{32\pi^2 l^4} \int_0^\infty \int_1^\infty \frac{x^3}{p^2} \left\{ \left[\frac{(s_1 + p)(s_2 + p)}{(s_1 - p)(s_2 - p)} \exp x - 1 \right]^{-1} + \left[\frac{(s_1 + \varepsilon_1 p)(s_2 + \varepsilon_2 p)}{(s_1 - \varepsilon_1 p)(s_2 - \varepsilon_2 p)} \exp x - 1 \right]^{-1} \right\} \mathrm{d}p\,\mathrm{d}x\,,$$

$$\varepsilon = \varepsilon\left(\frac{\mathrm{i}xc}{2pl}\right), \quad s = \sqrt{\varepsilon\left(\frac{\mathrm{i}xc}{2pl}\right) - 1 + p^2}\,.$$

[4] If the interaction potential of two molecules is $U = -c/r^6$, the total energy of pair interactions of all the molecules in two half-spaces separated by a gap l is $u = -(c\pi N^2)/12l^2$, while force f is defined as a derivative:

$$-f = -\frac{\mathrm{d}u}{\mathrm{d}l} = -\frac{c\pi N^2}{6l^3}\,.$$

It represents the correspondence between formulas (12) and (13).

Because of the presence of $\exp x$ in the denominators, the main contribution to the integral over $\mathrm{d}x$ comes from $x \sim 1$; so, since $p \geqslant 1$, the argument of the function ε for large l is close to zero over the whole significant range of values of the variables. In accordance with this circumstance, we may simply replace ε_1 and ε_2 by their values at $\omega = 0$, i.e., by the electrostatic permittivities which we denote by ε_{10} and ε_{20}, respectively. In metals, $\varepsilon(\omega)$ tends to infinity as $\omega \to 0$; therefore, it should be assumed for them that $\varepsilon_0 = \infty$.

In this way, we obtain

$$f = \frac{\hbar c}{32\pi^2 l^4} \int_0^\infty \int_1^\infty \frac{x^3}{p^2} \left\{ \left[\frac{(s_{10}+p)(s_{20}+p)}{(s_{10}-p)(s_{20}-p)} \exp x - 1 \right]^{-1} + \left[\frac{(s_{10}+\varepsilon_{10}p)(s_{20}+\varepsilon_{20}p)}{(s_{10}-\varepsilon_{10}p)(s_{20}-\varepsilon_{20}p)} \exp x - 1 \right]^{-1} \right\} \mathrm{d}p\,\mathrm{d}x\,, \quad (14)$$

$$s_0 = \sqrt{\varepsilon_0 - 1 + p^2}\,.$$

Here, the attractive force turns out to be inversely proportional to the fourth power of distance. Remarkably, it depends only on the electrostatic values of the permittivities of both interacting bodies.

Let us consider some special cases of formula (14). In particular, a simple result is found for two metals. Setting $\varepsilon_{10} = \varepsilon_{20} = \infty$ in formula (14) leads to

$$f = \frac{\hbar c}{16\pi^2 l^4} \int_0^\infty \int_1^\infty \frac{x^3\,\mathrm{d}p\,\mathrm{d}x}{p^2(\exp x - 1)} = \frac{\hbar c}{l^4}\frac{\pi^2}{240}\,. \quad (15)$$

This force does not depend in any way on the nature of the metals (which is not the case for 'small separations', where the strength of the interaction depends on the function $\varepsilon(\mathrm{i}\xi)$ at all ξ values, and not just at $\xi = 0$). Notice that formula (15) was obtained earlier by Casimir using a different method [18].

Here is the calculated result for two identical dielectrics ($\varepsilon_{10} = \varepsilon_{20} = \varepsilon_0$) obtained from formula (14) by numerical integration:

$$f = \frac{\hbar c}{l^4}\frac{\pi^2}{240}\left(\frac{\varepsilon_0 - 1}{\varepsilon_0 + 1}\right)^2 \varphi_{\mathrm{DD}}(\varepsilon_0)\,, \quad (16)$$

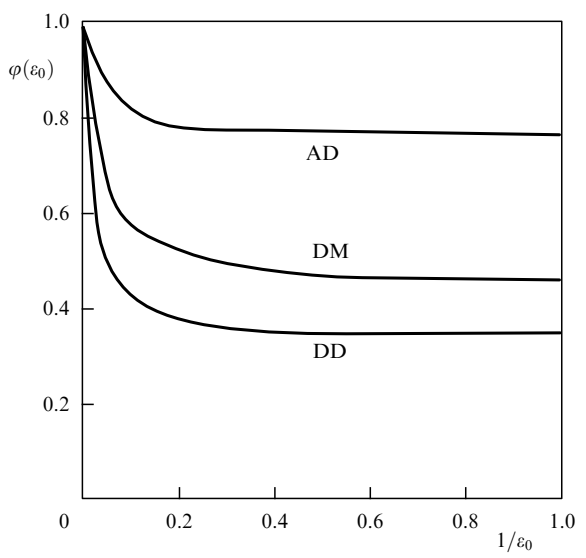

Figure 1.

where $\varphi_{\mathrm{DD}}(\varepsilon_0)$ is a function, the values of which are presented in Fig. 1. For $\varepsilon_0 \to \infty$, this function tends to unity [in accordance with formula (15)], and for $\varepsilon_0 \to 1$ it approaches 0.35, corresponding to the limiting law (18) (see below). The latter limit is practically reached at $\varepsilon_0 \approx 4$, after which φ_{DD} remains virtually constant.

The same figure depicts the curve of a similar function which gives the force of attraction between a metal and a dielectric ($\varepsilon_{10} = \infty$, $\varepsilon_{20} = \varepsilon_0$):

$$f = \frac{\hbar c}{l^4}\frac{\pi^2}{240}\frac{\varepsilon_0 - 1}{\varepsilon_0 + 1}\varphi_{\mathrm{DM}}(\varepsilon_0)\,. \quad (17)$$

Finally, let us carry out the passage to interaction of individual molecules in formula (14). To do this, we assume, as above, that both media are sufficiently rarefied, i.e., that the differences $\varepsilon_{10} - 1$ and $\varepsilon_{20} - 1$ are small. Keeping only the first nonvanishing terms in the expansion of the integrand in powers of these differences and carrying out the integration yield

$$f = \frac{\hbar c}{l^4}\frac{23}{640\pi^2}(\varepsilon_{10} - 1)(\varepsilon_{20} - 1)\,. \quad (18)$$

This force corresponds to the interaction of individual pairs of molecules with the potential energy

$$u(r) = -\frac{23\hbar c}{64\pi^3 r^7}\frac{(\varepsilon_{10} - 1)(\varepsilon_{20} - 1)}{N^2} = -\frac{23\hbar c}{4\pi r^7}\alpha_1\alpha_2\,,$$

where α_1, α_2 are the static polarizabilities of molecules ($\varepsilon_0 = 1 + 4\pi N\alpha$).

This formula coincides with the result obtained by Casimir and Polder [17] for van der Waals forces, including retardation effects; we have here obtained it from macroscopic considerations.

A similar limiting transition to the case of one rarefied medium and one arbitrary medium gives the energy $u(l)$ of interaction of a molecule with a solid wall from which the molecule is separated by distance l. In this case, only one of the differences, $\varepsilon_{10} - 1$ or $\varepsilon_{20} - 1$, in formula (14) must be regarded as small (let it be the first one).[5] As a result, we obtain the formula

$$u(l) = \frac{3\hbar c\alpha_1}{8\pi l^4}\frac{\varepsilon_{20} - 1}{\varepsilon_{20} + 1}\varphi_{\mathrm{AD}}(\varepsilon_{20})\,, \quad (19)$$

where

$$\varphi_{\mathrm{AD}}(\varepsilon) = \frac{1}{2}\left(\frac{\varepsilon + 1}{\varepsilon - 1}\right)\left\{\frac{2}{3} + 2\varepsilon + \frac{4 - \sqrt{\varepsilon}(\varepsilon + 1)}{\varepsilon - 1} - \frac{\operatorname{Arsh}\sqrt{\varepsilon - 1}}{(\varepsilon - 1)^{3/2}}\left[1 + \varepsilon + 2\varepsilon(\varepsilon - 1)^2\right] + \frac{2\varepsilon^2}{\sqrt{\varepsilon + 1}}\left(\operatorname{Arsh}\sqrt{\varepsilon} - \operatorname{Arsh}\frac{1}{\sqrt{\varepsilon}}\right)\right. . \quad (20)$$

As $\varepsilon_{20} \to \infty$, the function $\varphi_{\mathrm{AD}}(\varepsilon_{20})$ tends to unity and expression

$$u(l) = \frac{3\alpha_1\hbar c}{8\pi l^4}$$

[5] A similar transition is also possible in formula (10) for 'short separations'. However, for a practical calculation of the energy of interaction between an atom and a solid wall at these distances, it is again necessary to know the optical properties of the atom and the body in a wide spectral range.

coincides with the result of Casimir and Polder obtained by a different method for the interaction of an atom with a metal wall [17]. For $\varepsilon_{20} \to 1$, one finds $\varphi_{\mathrm{AD}} = 23/30 = 0.77$ (see Fig. 1).

A natural question arises as regards the actual value of λ_0 with which distance l should be compared. The answer cannot be given in the general form depending on the concrete shape of the spectral distribution of absorption in the given bodies, i.e., the concrete properties of function $\varepsilon''(\omega)$.

Specifically, a reasonable estimation of the applicability region of formula (15) for metals is possible by taking $\varepsilon(\omega)$ in the form

$$\varepsilon(\omega) = -\frac{4\pi e^2 N}{m\omega^2}\,, \tag{21}$$

where N is the number of conduction electrons per cm^3; this formula is known to hold for the infrared spectral region. Equation (21) leads to

$$\varepsilon(\mathrm{i}\xi) = \frac{4\pi e^2 N}{m\xi^2}\,;$$

the use of this expression in general formula (9) and the expansion of it in powers of $1/l$ give

$$f = \frac{\hbar c}{l^4}\,\frac{\pi^2}{240}\left[1 - 7.2\,\frac{c}{el}\sqrt{\frac{m}{N}}\right]. \tag{22}$$

At $N = 5.9 \times 10^{22}$ cm^{-3} (for silver), the second term in the brackets is small if $l \gg 0.6$ μm.

The case of quartz has certain peculiarities by virtue of specific properties of its absorption spectrum. Quartz is known to strongly absorb in the ultraviolet (starting at roughly 0.15 μm) and infrared (starting at a few μm) regions, being transparent between them. The distances of interest in the experiments of Abrikosova and Derjaguin fall into the transparency range, and l can be considered, for estimation purposes, to be smaller than $\lambda/2\pi$ at the right edge of the absorption region, and bigger than $\lambda/2\pi$ at its left absorption edge.[6] The contribution from the UV absorption region to the force f can be estimated from formula (16), assuming ε_0 to be equal to the refractive index squared in the optical transparency region. The contribution from the IR region is given by formula (10); to an order of magnitude, it is smaller by a factor of $l\omega_0/c$ (ω_0 are the IR absorption frequencies). Thus, a reasonable estimate of the attractive force f can be found from formula (16) with the optical (instead of electrostatic) value of permittivity as ε_0. The result is an underestimation on the side of long distances, and an overestimation on the side of short distances.

In the foregoing, we neglected the influence of body temperature T on the attractive force, i.e., the formulas were written out at $T = 0$. Such neglect is usually justified. It requires in the first place that the inequality $kT \ll \hbar\omega_0$ be satisfied, where ω_0 are the frequencies corresponding to the wavelengths λ_0. This condition is wittingly fulfilled at usual temperatures, which ensures the applicability of the above results for 'short separations'. In the case of a 'large separation', the condition may prove insufficient. An analysis showed that the following condition must be fulfilled, too:

$$kT \ll \frac{\hbar c}{l}\,.$$

It is apparently violated at sufficiently large distances l when the influence of temperature comes into prominence. This fact is crucial, even though the force f itself becomes very small at such distances.

We do not present here a general formula for the attractive force at any l and T values, as a generalized variant of expression (9). It is worthwhile to mention, for no other reason that to illustrate the temperature effect, that in the inverse limiting case of $l \gg \hbar c/kT$ the attractive force takes the form

$$f = \frac{kT}{8\pi l^3}\left(\frac{\varepsilon_0 - 1}{\varepsilon_0 + 1}\right)^2. \tag{23}$$

Thus, there is again an inverse cube relation when the distances are sufficiently large, but with a coefficient depending on temperature (and with electrostatic permittivity).

4. Experimental procedure [7]

4.1 Principle of measurement

The aforesaid makes clear the importance of devising a method for direct experimental determination of the distance dependence of attractive forces acting between solid bodies. This goal can be attained by specifying various distances H between the two bodies in sequential measurements and keeping them constant in each concrete measurement despite the action of the molecular force F tending to decrease them.

If one body is fixed to be motionless and another rigidly attached to a dynamometer or a balance that allows the force to be determined from the shift of the equilibrium position ΔH, the main difficulty arises from the fact that the distance dependence of the molecular force, i.e., the large positive values of the force gradient, may be responsible for the instability of the equilibrium position of the moving body.

Indeed, the instability condition implies that

$$g - \frac{\mathrm{d}F}{\mathrm{d}H} > 0\,,$$

where g is the dynamometer directing force (rigidity factor). Since $\mathrm{d}F/\mathrm{d}H$ is always positive,[8] the stability condition can easily be violated at small g, i.e., for a highly sensitive instrument. In contrast, if $\mathrm{d}F/\mathrm{d}H < g$ over the entire range of H values being studied, $\mathrm{d}F/\mathrm{d}H$ for the upper boundary of the interval is much smaller than g. Because $F \sim -H^{-k}$ and therefore $\mathrm{d}F/\mathrm{d}H = k(F/h)$, where $k \geqslant 2$, the equilibrium shift ($\Delta H = F/g$) under the action of the force makes up only a small fraction of the gap H between bodies, which makes measurements difficult.

On the other hand, the use of a rigid dynamometer or a 'coarse' balance has an advantage, since it shortens the balance vibration period and reduces the influence of viscosity of the air layer filling the narrow gap between both bodies, which serves as a vibration damper.

[6] Results of a special study give reason to conclude that the characteristic criterion is the comparison of l with $\lambda/2\pi$ rather than with the wavelengths themselves in the absorption regions.

[7] We acknowledge the participation of F B Leib in the elaboration of this method.

[8] Assuming the attractive force to be negative.

These conflicting requirements were reconciled by using the movement of the body as an indicator not of the force acting on it (for which purpose a different parameter is applied) but of the deviation of the distance between it and the immovable body from the set value. By keeping watch on such an 'indicator', it is possible to automatically maintain the distance constant, e.g., by passing a current of the proper strength and direction through the coil connected with the body and placed in a magnetic field. The maintenance of a constant gap between both bodies by such 'remote control' of the position of one of them is possible only if the molecular force of interest acting on it is at the same time balanced by an electromagnetic force. In other words, the method in question represents a compensation method.

At the same time, it is obvious that such a compensation performed manually and based on visual observations (e.g. of interference rings in the gap between the bodies) does not guarantee reaching the needed stability of the gap, because the reaction of the experimentalist is too slow and the sensitivity to variations of the gap width is insufficient.

The problem is resolved by automating the measurements with the employment of a special apparatus consisting of a highly sensitive device (detector) to track changes in the body position and regulate the current in the coil.

Such an automated compensation measuring scheme simultaneously exemplifies a self-oscillatory system with a feedback. If the current strength is considered to be a system coordinate influencing the body position (viewed as a dependent coordinate) by virtue of the moment proportional to the current, the tracking device measuring the current strength as a function of body position effects a sort of negative feedback capable of maintaining the stability of the system's equilibrium position. It is easy to make the oscillation period very small and the damping very large [9] by preventing induction of self-oscillations. In other words, the proposed principle of measurement keeps the gap width constant and at the same time ensures compensation measurements of the molecular attractive force.[10] From what follows, it will be clear that this scheme has still more advantages, e.g., high sensitivity in a short natural period and elimination of the influence of viscosity of the air layer between the bodies, as well as prevention of zero-creep. Notice that an analogous automated compensation device can be connected with a galvanometer to increase its sensitivity and shorten the period.

These examples show that automation of measurements by using a more intricate setup with feedback instead of a simple one and other means of control is, in fact, an application of cybernetics worthy of further systematic development in view of the promising possibilities it offers.

A device based on the above general principle of measurement is described in the next section together with the measuring procedure [27–34].

[9] By introducing in the circuit a phase shifter that makes the current phase lead the body position variation phase.

[10] A similar scheme also provides a number of advantages for measuring specially constant forces, such as weight. One of us [26] suggested to apply as feedback not a tracking device but a device ensuring the action of a moment proportional to the current on the balance beam. It certainly introduced a measurement error, even if not a fundamental one. Note that such a device employed with a balance for weighing a constant load is at the same time a precise current stabilizer.

4.2 Objects of measurement

For various reasons, it is convenient to shape one object as a flat body, and another as a sphere and measure the force of attraction between a plate with dimensions of 4×7 mm and spherical lenses having radii of curvature $R = 10$ cm and $R = 25$ cm. Such a choice makes it easier to adjust surfaces than in the case of two plates; moreover, the shortest distance between the bodies can be simply and accurately calculated from Newton ring diameters. Also, the viscous drag in the air layer between solid surfaces decreases in proportion to R^2. Finally, such objects make it possible to examine the dependence of the forces on the radius of curvature of the spherical surface and thereby to distinguish between the molecular forces proportional to the radius of the spherical surface and various masking effects, e.g., those associated with surface electrization. The relation giving the proportionality between the molecular attraction (according to any law) and the radius of the sphere was derived by Hamaker [21] as

$$F(H) = 2\pi R u(H)\,, \tag{24}$$

where $F(H)$ is the attractive force between the sphere and the flat plate, R is the radius of the sphere, $u(H)$ is the interaction energy per cm^2 between two infinite plates of the same nature and in the same medium, and H is the shortest distance between the surfaces. It follows from this formula as well that experiments on measuring the attractive force between the sphere and the flat plate give directly the energy of interaction between two infinite flat plates, unrelated to the radius of curvature R.

The material used for the samples was generally quartz glass resistant to reagents that can be made to have a perfectly smooth surface.

Because the force of attraction between macroscopic objects is small, it is also desirable to fabricate samples from materials characterized by strong interaction forces, other things being equal. It follows from Lifshitz's theory that interaction forces at large enough distances between the objects depend only on the electrostatic value of permittivity ε_0. Of the dielectrics with intrinsically high ε_0, thallium halides proved most suitable for our purpose. We carried out a series of measurements addressing interaction forces between a plate and a lens of a mixed crystal containing 42.5% thallium bromide and 57.5% thallium iodide.

The highest interaction force and the simplicity of calculation make metals an interesting object of study. Technically, a combination of a metal and a transparent dielectric provides the simplest case, because it allows us to retain the optical method for measuring the gap. Therefore, we took advantage of a lens from quartz glass and coated a quartz plate with a chromium layer (by vacuum deposition). A relatively low reflectivity of the chromium surface makes it possible to observe rather contrasting interference rings in the gap between metal and quartz surfaces.

Measurements of the attractive force between the two objects were made in air and vacuum. The interaction between two bodies must not strongly depend on what is in the gap between them, whether vacuum or air, but each has advantages and disadvantages from the experimental and methodological point of view, the comparison of results obtained in each case being an important tool for controling the correctness of the measurements. Vacuum experiments proved to be a more accurate and convenient modality, because the air viscosity forces in the gap between the

surfaces, even when its variations proceed slowly, may become comparable to the molecular forces being studied. For this reason, measurements in the air had to be performed waiting for the gap to be constant before readings. Therefore, the measurement procedure was protracted and frequently could not be synchronized with the moments free from oscillations, despite the sharp decrease in the natural oscillation period by applying negative feedback. Moreover, it was impossible to completely avoid beam vibrations caused by convective flows in the air experiments. Such interferences were less pronounced in the vacuum experiments, when the residual air pressure varied from 1×10^{-1} mmHg to several mmHg.

4.3 Feedback microbalance for measuring the interaction force between solid bodies

Balance beam. The interaction force between the flat-plate surface P and the convex lens surface L was measured using a special beam-type microbalance (Fig. 2) following the automated compensation scheme expounded in a preceding section. The beam K was 35 mm long and weighed 0.1 g. The plate P was placed on one end of the beam, and the lens L was mounted on an independent support so that the distance between its downward convex surface and the top surface of the plate was sufficiently short. A small mirror S was cemented to the other end of the beam. An agate prism 'a' that rested on an agate block 'b' was attached to the beam. A glass rod C weighing 10–50 mg and moving like a rider along the beam served for rough balancing. The beam was rigidly fixed to the frame R with 15–20 turns of wire placed in a constant magnetic field with $B \approx 850$ G (Fig. 3).

Compensating and tracking devices. The measured molecular attraction was compensated by passing through the frame R a current supplied by Wollaston wires 6–10 μm in diameter. The current source was the tracking device (a beam rotation sensor consisting of a raster photorelay and a single-cascade amplifier). The relay was arranged above the beam so that its optical axis OO (Fig. 4) was parallel to the beam rotation axis. The raster photoelectric sensor is schematically depicted in Figs 3 and 4.

The condensing lens K directed the rays from the light source L (a 50-W incandescent lamp) toward a linear (typographic) raster P_1 (a glass plate with alternating transparent and opaque strips of equal width). The rays passed through the objective O_1 and were focused on the mirror S as shown by the solid line. The objective O_1, the mirror S, and the second objective O_2 with the same focal length (7.5 cm) served to throw the real image of raster P_1 upon the plane of the second raster P_2 with the same screen ruling of 60 lines per cm (broken line). The image size of raster P_1 coincided with that of raster P_2, because both were located in the focal planes of identical objectives O_1 and O_2. The raster planes were perpendicular to the plane containing the beam rotation axis and the balance beam itself; the raster lines were perpendicular to these. The slightest turn of the mirror changed the position of the first raster image relative to the second raster, increasing or decreasing the amount of light transmitted. After passing through the second raster, the light reached an antimony–cesium vacuum photocell which controlled the grid of the amplifier valve. Some experiments used an autocollimation arrangement for the raster photorelay (Fig. 5). The filament of the 50-watt lamp L was placed in the focal plane of the objective O_1 (focal length 5 cm). Parallel rays passed through the right half of the raster P were focused by the objective O_2 (focal length 5 cm) on the mirror S. By reflection from S, an image of the raster was produced in the

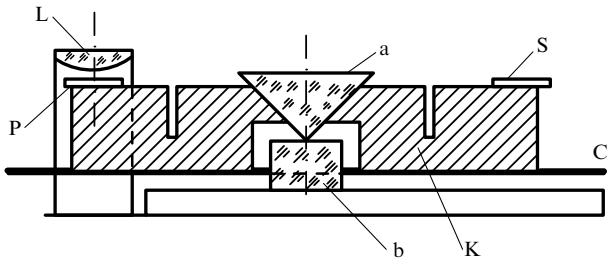

Figure 2.

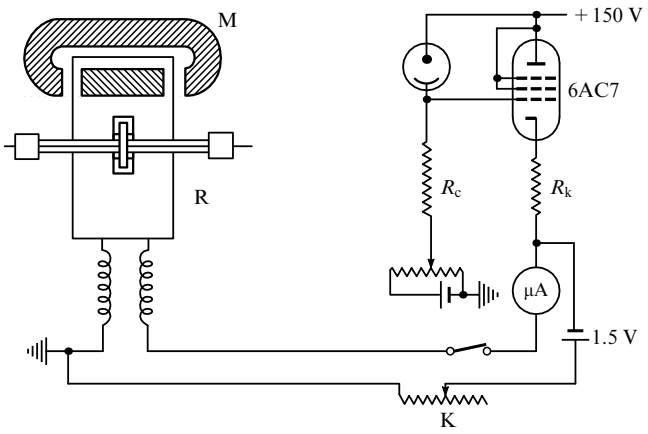

Figure 3.

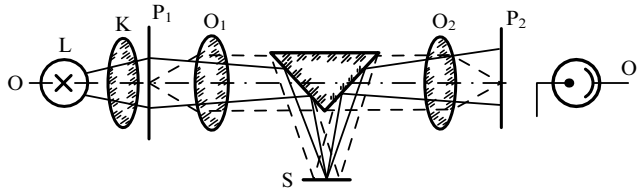

Figure 4.

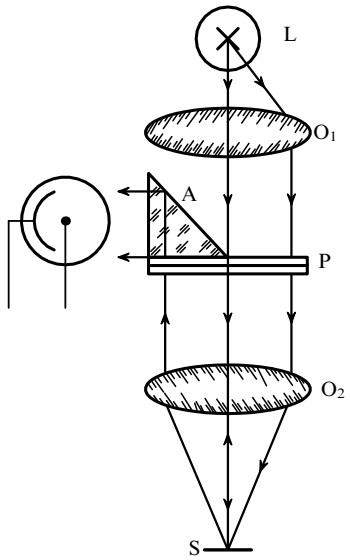

Figure 5.

plane of a P itself (left-hand side). The parallelism of the rays ensured an optical imaging scale of 1:1. Immediately beyond the raster was a total internal reflection prism A whereby the light reflected from the mirror reached a photocell, with the illumination depending on the position of S. The raster P was cut in half along the rulings. One half was moved relative to the other in a direction perpendicular to the rulings using a differential screw. This arrangement made it possible to adjust the gap between bodies by the method described below.

The photocell current was amplified by the simple scheme shown in Fig. 3. A battery giving a negative grid bias was included through a potentiometer in the circuit of the 6AC7 valve grid. The negative feedback in the amplifier (cathode resistance R_c) ensured good stability of its operation. An anode current i partly compensated by the current i_1 from a dry battery with $E = 1.5$ V was passed to the balance frame R. Changing i_1 by means of the resistance box K permitted the current in the frame to be adjusted, while remaining on the steepest part of the amplifier valve characteristic.

Design of the apparatus. Figure 6 demonstrates the design of the apparatus exploited. A massive brass plate *1*, to which all the component parts are attached, rests on three supports whose height is such that the control screws can be operated where they project from under the plate. On the plate itself are another plate *1′* carrying the balance beam *2*, the lens support *3*, the mechanism *4* for moving the glass hair, the stop *5*, the magnet *6*, its core *7*, and supports *8* for anchoring the raster relay. The plate *1′* has been set upon three supports. The height of two of them can be altered by means of differential micrometric screws located under the plate *1*. The purpose of this will be explained below. An agate block 'b' serving as a support for the agate knife edge 'a' of the beam was adhered to the plate (see Fig. 2).

The balance beam was fabricated of aluminum 0.16 mm thick in the form of a Π-shaped channel. Three recesses were made in it: the middle one to carry the agate prism fixed with shellac, and the other two for the glued frame R. The rectangular base of the frame was made of 0.16-mm thick aluminum with a strengthening rib. The ends of enameled copper wire 50 μm thick wound on the frame were soldered to thin Wollaston wires brought out to the terminals *13* beneath the glass rod movement mechanism. The mirror S and the plate P in question were fixed to the ends of the beam with aluminum connectors. An aperture was made in the plate *1′*, with the lens support passing freely through it.

The plate screws previously mentioned served to tilt the balance beam with the plate at various angles to the lens, which was necessary in order to displace the point of contact between the surfaces being studied.

The glass rod *9* used for rough balancing out and for calibration rested in the channel of the beam and was displaced along it by the slider *10*. The slider was moved in turn by a screw projecting from under the plate, which imparted motion to the horizontal carriage *4*.

To prevent contact between the lens and the plate, and to detach them from one another in the case of deliberate or accidental contact, a special stop *5* was designed. The contact between the stop and the beam was established through the crossed edges of two corundum crystals (to reduce the adhesion forces), one adhered to the left-hand connector, the other to the stop plate. The stop was displaced vertically by means of a differential screw.

All parts of the apparatus between the photorelay fixing supports were covered with a shallow brass casing having glass windows above the beam mirror and the lens. In the vacuum variant of the apparatus, the casing was sealed to the plate with a rubber gasket, and all the micrometric screws transmitted movement through bellows. The supports *8* served for attaching the raster photorelay (see Fig. 4) mounted inside a brass tube.

The actual sensitivity of the apparatus for determining the interaction force depended considerably on the vibrations of the base whereat the apparatus was installed. These caused oscillations of the current in the circuit of the frame R. The oscillations were partly excited because the center of mass was not exactly at the point of support, partly by the transfer of rotational vibrations of the base to the beam through the viscous layer of air. The best results were obtained by placing the apparatus on a damping table (*11* in Fig. 6), which in turn was located on a cement plinth isolated from the foundations and embedded in the ground (*12* in Fig. 6).

In order to further reduce the influence of vibrations, the optical scheme of the detector was improved. The light reflected from the mirror S_1 (Fig. 7) attached to the beam was further reflected from the mirror S_2 attached to the plate (*1* in Fig. 6), thus making the photocurrent independent of the vibrations of the balance beam with the plate as a whole and dependent only on the gap H. The angle between mirrors S_1

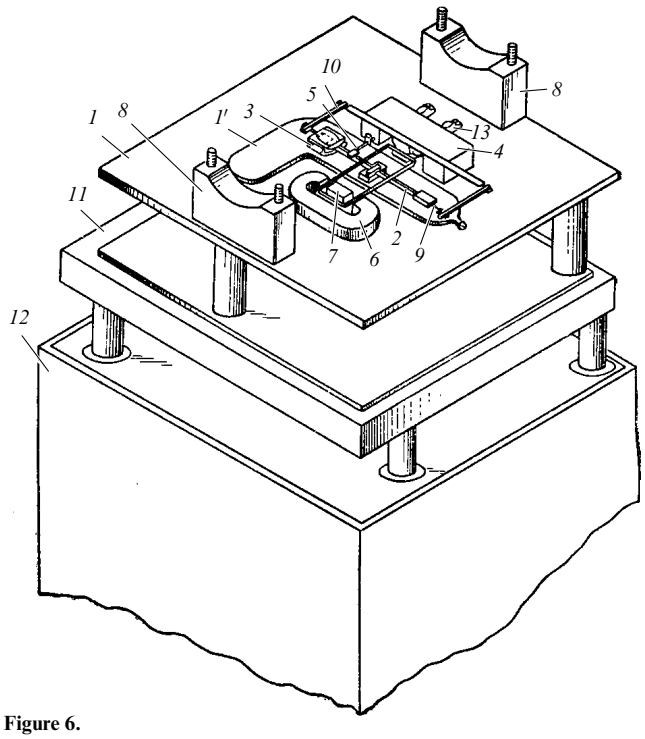

Figure 6.

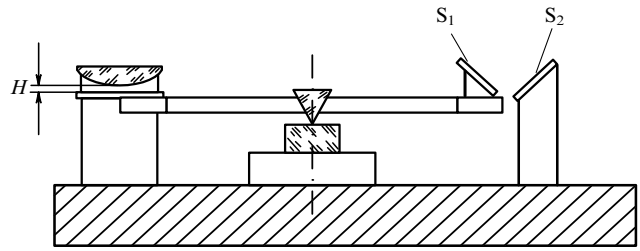

Figure 7.

and S_2 was around 90°. The position of the mirrors could be adjusted when setting up the apparatus by means of a screw projecting from beneath the plate.

Measurement procedure. Let us first consider a position of the balance beam for which the gap between the plate and the lens is so great that the molecular attraction is imperceptible. We assume that the center of mass of the balance almost leveled with the supporting edge of the beam is displaced horizontally relative to it.[11] A certain current i_0 must then be passed through the frame for the purposes of balancing. This can be done for a given position of the beam by setting with the aid of the microscrew the raster P_1 (Fig. 4) in a position such that the required amount of light passes through the relay to the photocell. When the gap H is varied, i.e., by changing the position of the beam and its attached mirror, the same i_0 is needed for balancing and therefore the same light flux, provided it is possible to neglect the horizontal displacement of the center of mass when the beam rotates. In the measurements, it was always possible to satisfy this condition, when H varied from 1 to 20 μm. In order to keep the light flux constant when the beam with the mirror rotates, the raster P_1 has to be displaced to a new position.

It is therefore evident that, by slowly moving the raster in the appropriate direction, the beam will be made to undergo a slow change in its equilibrium position to reduce the gap H. This is, of course, possible so long as the equilibrium position resulting from the compensation will be stable. For this, it is necessary that the change in the photocurrent when the beam rotates cause, by the negative feedback via the raster relay, a force opposing the motion of the beam. To achieve this, it is sufficient to make the correct choice of the direction in which the current passes through the turns on the frame. Thus, by acting on the tracking system or, rather, on the raster P_1 that is part of it, one could control the balance beam. In so doing, the beam rotation was not accompanied by any change in the current [12] if the center of mass of the balance was leveled with its axis of rotation and no other forces were acting. The situation is changed if the gap is made so small that molecular attraction manifests itself. In order to compensate, a different value of i_0 is needed and is automatically provided by the feedback if the equilibrium reached is stable.

The stability condition is given by

$$\frac{1}{r^2}\frac{\mathrm{d}i}{\mathrm{d}\alpha}\frac{\mathrm{d}M}{\mathrm{d}i}-\frac{\mathrm{d}F}{\mathrm{d}H}>0\,,$$

where $\mathrm{d}i/\mathrm{d}\alpha = k$ is the derivative of the amplifier output current with respect to the beam rotation angle α, which is determined by the sensitivity of the photorelay and could be easily brought to very high values on the order of 500 A rad^{-1}, and r is the distance between the point of closest approach of the plate to the lens and the beam rotation axis; $\mathrm{d}M/\mathrm{d}i = n$ was made small, since the force measurement sensitivity (unlike current measurement with the galvanometer) is obviously inversely proportional to $\mathrm{d}M/\mathrm{d}i$. The frame was shunted in order to increase this sensitivity. However, it is impermissible to reduce n greatly, thus decreasing $\mathrm{d}M/\mathrm{d}\alpha = l = kn$, since this makes the vibration period of the beam with feedback extremely large, if gravity is neglected, and equal to

$$T = 2\pi\sqrt{\frac{J}{\mathrm{d}M/\mathrm{d}\alpha}}\,,$$

with J being the moment of inertia of the beam. In the limit, the stability of the beam may break up.

It is clear from the above how we can determine, by turning the beam with the aid of the raster P_1 displacement and noting the values of i_0 for various gap sizes H, the dependence of the molecular interaction of the plate and the lens on H if we know the proportionality factor between the force and the current, which is

$$\frac{1}{r}\frac{\mathrm{d}M}{\mathrm{d}i}=\frac{n}{r}\,.$$

Besides the photocell current, we can use in the same circuit the additional current from the battery; this is particularly important when measuring large forces.[13]

Balance alignment, adjustment, and calibration. The zero current i_0 is constant only when the intrinsic guiding moment M_0 of the balance without feedback is much less than the moment M. Naturally, $M_0 = 0$ when the distance d between the center of mass and the point of support (in this case, the prism edges) is zero. Applying feedback that determines the oscillation period and that can make it sufficiently small, one can (in contrast to an ordinary balance) reduce d arbitrarily close to zero. In the balance described, the center of mass resided almost on the knife edge of the prism. The criterion for d to be sufficiently small was the constancy of current i_0 in the frame over a wide range of spatial positions of the beam, of course when H is so large that no interaction forces occur between the plate P and the lens L.

It was found that i_0 remains constant, with an accuracy entirely sufficient for these measurements (0.1 μA or less), when $d \leqslant 0.025$ mm corresponding to the vibration period (without feedback) $T_0 \geqslant 6$ s. These characteristics are very sensitive to smallest changes in the balance, so that it was necessary to reestablish the proper values of $T \geqslant T_0$ or $d \leqslant d_0$ before each experiment. The glass rod C (Fig. 2) of an appropriate weight was chosen in order to achieve these conditions.

The positioning of the center of mass on the knife edge considerably reduces the sensitivity of the apparatus to vibrations of the base, since they are transmitted mainly through the supporting point.

Since there is direct proportionality (with the coefficient n) between the current strength and the electromagnetic moment of the interaction between the frame and the magnet, the sensitivity of the balance with feedback is independent of the sensitivity and other properties of the detector; the balance provides a linear relation between the force of interaction of the bodies ('load') and the frame current with either a linear or a nonlinear amplifier characteristic. Such a balance allows the sensitivity to be adjusted by changing the number of turns on the frame and the magnetic field strength, or by simply shunting the frame.

[11] The horizontal displacement of the center of mass was effected by moving the rod C (Fig. 2), but it was very difficult, and actually unnecessary, to make the centers of mass coincide exactly.

[12] There are viewed only some deflections of the pointer of a galvanometer, placed in the circuit of the frame, from the position i_0, when the raster and the beam carried by it displace rapidly. These deflections are quickly damped when the displacement is stopped or considerably slowed down, indicating that the air layer exerts a viscous drag on the gap variation.

[13] In particular, such a compensation scheme has been used for feedback with a microanalytical balance in our work with T N Voropaeva, and with K K Timofeev and Yu N Sachkov of the Balance and Instrument Research Institute (Moscow).

The coefficient l and, therefore, the balance vibration period depend on the current yield k that can be varied over a wide range by means of various parameters of the amplifier circuit, changing the cathode resistance R_c (Fig. 3), working in different parts of the amplifier anode characteristic, or using an amplifier valve with a smaller slope.

When the negative feedback method is applied to an ordinary analytical balance, the slow creep of the current yield is not a hazard (unlike short-period fluctuations), because equilibrium is maintained by the gradual rotation of the beam, leaving constant (if the forces of inertia are small) the anode current from which the load is assessed.

When the molecular attraction is being 'weighed', both fast and slow changes in the detector are hazardous, for there needs to be a sufficiently prolonged stable equilibrium of the beam in order to measure at the same time the gap between the surfaces and the corresponding current. This is particularly important for measurements in air, since then the beam creep generates drag forces that depend on the air viscosity and perturb the forces measured.

With the method described, it was possible to measure the interaction forces between solids from about $(1-2)\times 10^{-4}$ dyn to 20 dyn, when the forces decreased fairly rapidly with increasing distance. For example, with large values of $l = kn$ (where the detector current yield k is about 500 A rad^{-1}) and a vibration period of 5×10^{-3} s, one can measure a force having a gradient of 10^6 dyn cm^{-1} with an accuracy down to 0.02 dyn.

As a result of these properties of the balance, it was possible to overcome the serious difficulties posed by the problem.

When the gap was large enough (tens of micrometers), large-amplitude self-vibrations of the balance beam were observed, resulting from the inertia of the feedback, namely, from the amplifier output current having a phase lag relative to the beam rotation. To remove such an effect, phase shifters can be connected in the circuit. However, with gaps below 20 μm, even in vacuum (10^{-2} mmHg) measurements, the damping action of the air layer was sufficient, and the use of phase shifters was not necessary.

The force of interaction between the lens and the plate was found as

$$F = \frac{n}{r}\, i = \gamma i\,,$$

where i is the current measured with a class 0.1 microampere-meter in the anode circuit (Fig. 3), and r is the distance measured with a rule between the knife edge of the prism 'a' and the point of closest approach of the surfaces; on the average, r was equal to 1.9 cm. The balance was calibrated (or n determined) by displacing the glass rod C (Fig. 2) along the beam. With a large gap between the surfaces (in the absence of molecular attractive forces), the microampermeter measured the current i_0 in the frame, corresponding to various positions of the rod as viewed on the eyepiece scale of the microscope.

The coefficient n is defined as

$$n = P\,\frac{\Delta y}{\Delta i_0}\,,$$

where P is the weight of the glass rod, Δy is its displacement, and Δi_0 is the corresponding change in the current.

To make the determination of n more exact, i_0 was plotted against y. Figure 8 shows one calibration graph giving $n = 2.51$ mg cm μA^{-1}, in good agreement with the value of

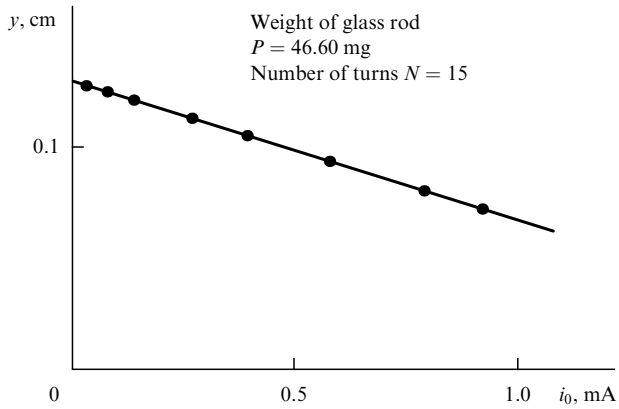

Figure 8.

$n = 2.55$ mg cm μA^{-1} calculated by Ampere's law from the magnetic field strength.

The accuracy of the latter calculation is certainly less than that of determining n from the calibration graph, and the calculation served mainly as a check. The error in the calibration determination of n was ±3% ($\gamma = 1.32 \pm 0.04$). The random errors in measuring the force F were about 10^{-4} dyn .

4.4 Method for measuring the distance between bodies

The minimum gap H between the lens L and the plate P was computed from the diameters of Newton's rings measured with a microscope equipped with an eyepiece scale. The system was illuminated with a 300-W filming lamp through a constant-deviation monochromator and the vertical illuminator of the microscope, which made the light reach the plate surface at normal incidence (Fig. 9).

Let d_m be the diameter of the mth dark ring, λ the light wavelength, and R the radius of the spherical surface. The formation condition of this interference ring is defined as

$$2\delta_m + 2H + \frac{\lambda}{2} = (2m+1)\,\frac{\lambda}{2}\,.$$

From geometrical considerations, the part of the air layer thickness denoted by δ_m (Fig. 10) is related to d_m by the formula

$$\delta_m = \frac{d_m^2}{8R}\,.$$

Replacing δ_m by d_m, we arrive at the formula

$$H = \frac{\lambda}{2}\left(m - \frac{d_m^2}{4R\lambda}\right) \tag{25}$$

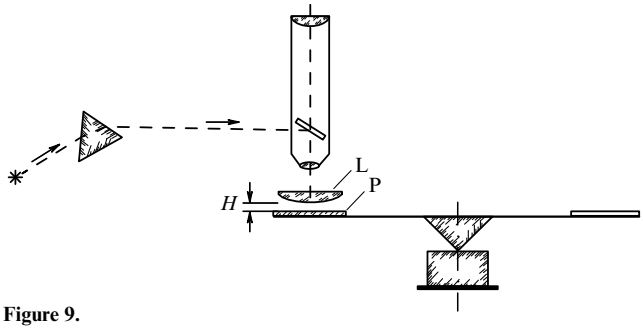

Figure 9.

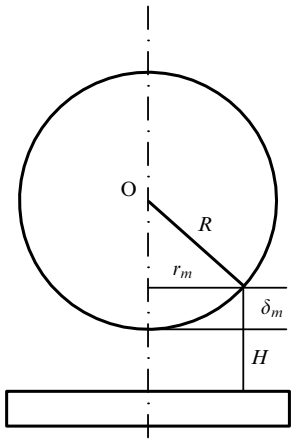

Figure 10.

for the minimum distance H between the surfaces, from which it follows that, in order to determine H, one needs to know m, d_m, λ, and R.

The ring number m can be determined by tracking the ring as the surfaces are brought into contact and counting off its serial number. This method is inconvenient for measuring molecular attraction between bodies because of the possibility of contact electrization. Another method was therefore applied based on measuring the interference ring diameters for various m and wavelengths λ of monochromatic light at a constant gap H.

Let us introduce quantities $\Delta(d_m^2)$ and $\Delta(d_\lambda^2)$ defined by the following relations:

$$\Delta(d_m^2) = d_{\lambda+\Delta\lambda,\,m}^2 - d_{\lambda,\,m}^2\,, \tag{26}$$

and

$$\Delta(d_\lambda^2) = d_{\lambda,\,m+\Delta m}^2 - d_{\lambda,\,m}^2\,. \tag{26$'$}$$

Taking into consideration relationship (25), we can write down the equalities

$$\frac{\Delta(d_m^2)}{\Delta\lambda} = 4Rm\,, \tag{27}$$

and

$$\frac{\Delta(d_\lambda^2)}{\Delta m} = 4R\lambda\,. \tag{27$'$}$$

Dividing formula (27) by (27′) leads to the expression for m:

$$m = \lambda\,\frac{\Delta(d_m^2)\,\Delta m}{\Delta(d_\lambda^2)\,\Delta\lambda}\,. \tag{28}$$

Before the beginning of the main measurements, i.e., of the attractive force F and the corresponding gap H, the last relation (28) was utilized to determine the number m of some ring and, from that, the numbers of the other rings.

The spherical surface radius R was measured with the same optical system. From expression (25), there is a linear dependence of d_m^2 on m at constant λ and H. If d_m^2 is plotted on the ordinate axis and m on the abscissa, the tangent of the angle between the straight line $d_m^2 = f(m)$ and the abscissa axis divided by 4λ gives radius R. Since λ, m, and R were always determined before the main measurements, they actually reduced to measuring the current i and the diameter of one (sometimes two or three) interference ring. This made the experiment easier to perform successfully by allowing attention to be concentrated on the simultaneous measurement of only two quantities.

In calculating the gap H between quartz and metallic surfaces, it was necessary to take into account the phase shift in reflection from the metal. For the chromium metal utilized in our experiments, this correction to H was about 120 Å.

The accuracy of the measurement of the gap width H was almost entirely dependent on the error in measuring the diameter d_m of the mth (usually the second) ring, which was $\pm 1\%$ (for d_2), ensuring an accuracy of roughly 0.01 μm in the measurement of H.

4.5 Preparation of the surfaces

If the experiment is to succeed, the surfaces must first be carefully cleaned to remove any film. The usual methods of chemical cleaning, such as washing with a chromium mixture, were not applied in order to avoid damaging the polished glass surface. To obtain a thorough cleaning, the plate and the lens were washed with distilled alcohol and ether using cotton wool degreased in a Soxhlet apparatus and then subjected to a glow discharge under a glasshood. The cleanness of the surfaces was confirmed by the fact that they could be completely wetted by water.

The most significant difficulties in the experiment arose from dust particles falling onto the surfaces studied and the charging of these when the particles were removed. The best results were obtained by rubbing the surfaces (after cleaning in the glow discharge) with degreased cotton wool slightly wetted with pure ether, while viewing the surface through a binocular microscope. After this treatment, the surfaces remained clean and completely wettable by water.

As dust particles were removed from the surfaces, strong electrization of the bodies took place, and they therefore interacted with a force that might be thousands of times greater than the molecular attraction. To remove the charges from the plate and lens surfaces, these had to be kept 1–10 mm apart and in some way the air near the apparatus ionized. It was impossible to remove the charges with the surfaces placing close together. The air was ionized with a radioactive sulfur isotope (S^{35}) placed nearby. When the surfaces were separated, dust particles were often deposited on them again from the air and they had to be cleaned and the charges removed repeatedly until both dust and electrostatic interaction were absent. Experience showed that with very small distances between the lens and the plate no dust enters the gap, and it was therefore important to achieve this once dust and charges on the surfaces are simultaneously absent, after which they should not be moved apart further than 5–10 μm.

5. Results of measurements

Figure 11 shows the dependence of the attractive force F measured in air between a quartz plate and a quartz sphere ($R = 10$ cm) on the gap width H.

It corresponds to the smallest attraction effect observed with objects of quartz glass. This dependence and the fairly good reproducibility of the effect in different experiments testifies to its molecular nature. However, to be sure that this view is correct, we need evidence that the experiments do not involve other attractive forces, especially electrostatic ones.

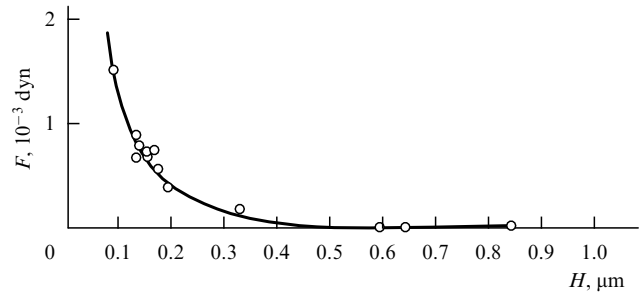

Figure 11.

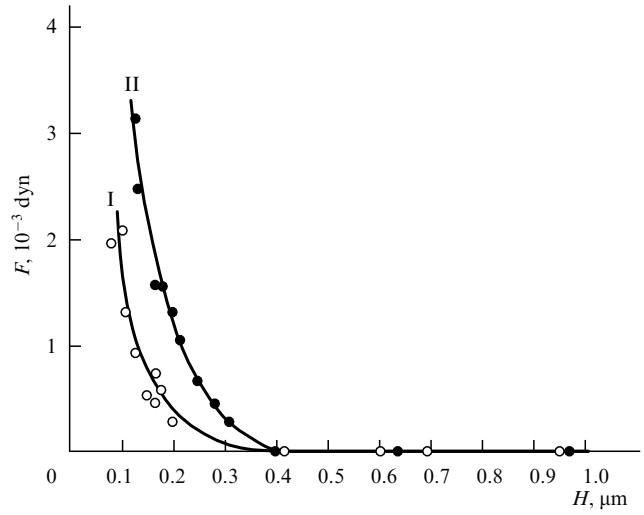

Figure 12.

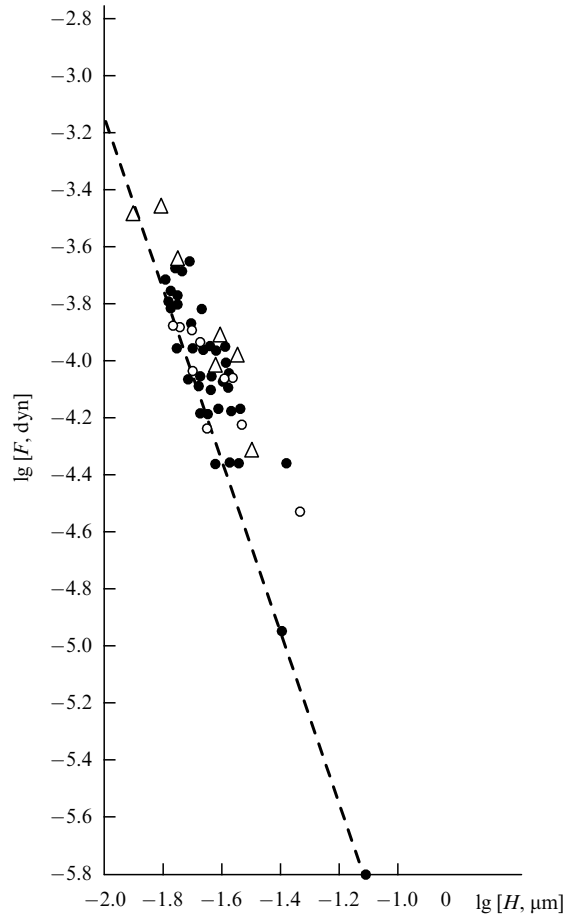

Figure 13.

If the observed attraction between the bodies has indeed molecular nature, it must be

(1) insensitive to repeated ionization of the air near the objects under measurement,

(2) proportional to the radius of the spherical surface (see formula (24)),

(3) readily reproducible between experiments both in magnitude and in force reduction with increasing distance,

(4) readily reproducible between experiments in relation to different points of approach of the interacting surfaces, and

(5) insensitive to the removal of air from the gap between the bodies.

Table 1.

$R = 10$ cm		$R = 26$ cm	
H, μm	$F \times 10^3$, dyn	H, μm	$F \times 10^3$, dyn
0.08	1.95	0.13	3.14
0.10	2.08	0.14	2.49
0.11	1.30	0.17	1.57
0.13	0.91	0.18	1.57
0.15	0.52	0.20	1.31
0.16	0.72	0.22	1.05
0.17	0.46	0.25	0.66
0.18	0.59	0.28	0.46
0.20	0.26	0.31	0.26
0.42	0	0.42	0
0.64	0	0.62	0
0.96	0	0.71	0
		0.96	0

Subsequent investigations sought to test the fulfilment of these conditions.

The most exact and reproducible measurements were taken in vacuum. The results are presented in Fig. 12 and Table 1. Curves I and II are for $R = 10$ and 26 cm, respectively. Within the error of measurement, these results satisfy all the above conditions.

Figure 13 gives a double logarithmic plot of the results obtained in a large number of experiments separated by considerable intervals of time and utilizing various quartz samples. The lens radius was $R = 11.1$ cm.

The white circles mark values measured in air. Before practically every measurement, the air near the bodies has been exposed repeatedly to powerful ionizers before evacuation. The broken lines in the diagrams were calculated from Lifshitz's theory (see below).

According to formula (24), the quotient obtained when the quantity $F(H)$ is divided by $2\pi R$, where R is the radius of the spherical surface concerned, is the attraction energy u per unit area between two infinite plates. Figure 14 depicts the dependence of u on spacing H, with the black circles, the triangles, and the white circles corresponding to experiments with lenses having $R = 11.1$, 10, and 25.4 cm, respectively.

This graph illustrates the linear dependence of the attractive force on the sphere radius, the attraction energy $u(H)$ for the plane case thus being independent of the lens used to measure the force. In other words, all the above conditions are satisfied.

Figures 15 and 16 demonstrate the results of experiments with samples prepared from thallium halides. Figure 15 is a

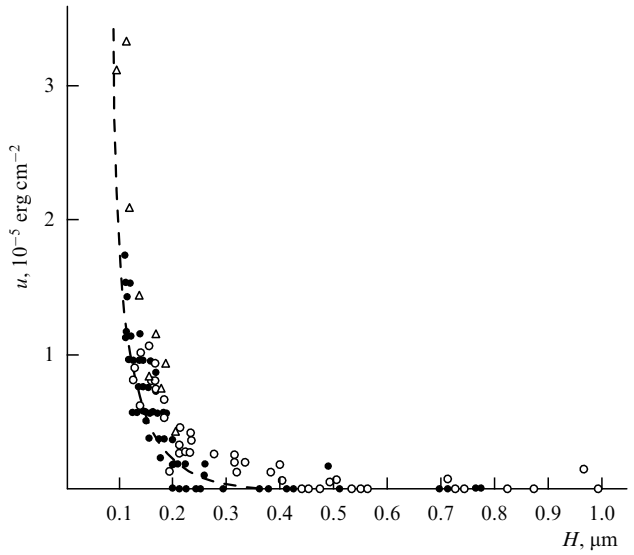

Figure 14.

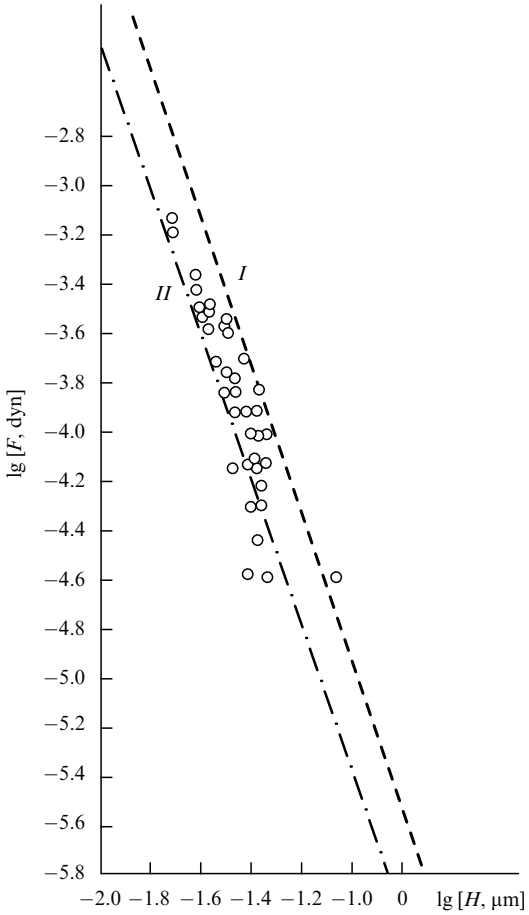

Figure 15.

double logarithmic plot of the data obtained with a lens having $R = 12.5$ cm; the circles and crosses in Fig. 16 represent the results of experiments with lenses of radius 12.5 cm and 5.2 cm, respectively.

Figures 17 and 18 are similar diagrams for the measurements in which one surface (the plate) was covered with a fairly thick mirror-surfaced layer of chromium. The values of the lens radius of curvature R are 10.6 cm in Fig. 17, and 10 cm (circles) and 5 cm (crosses) in Fig. 18.

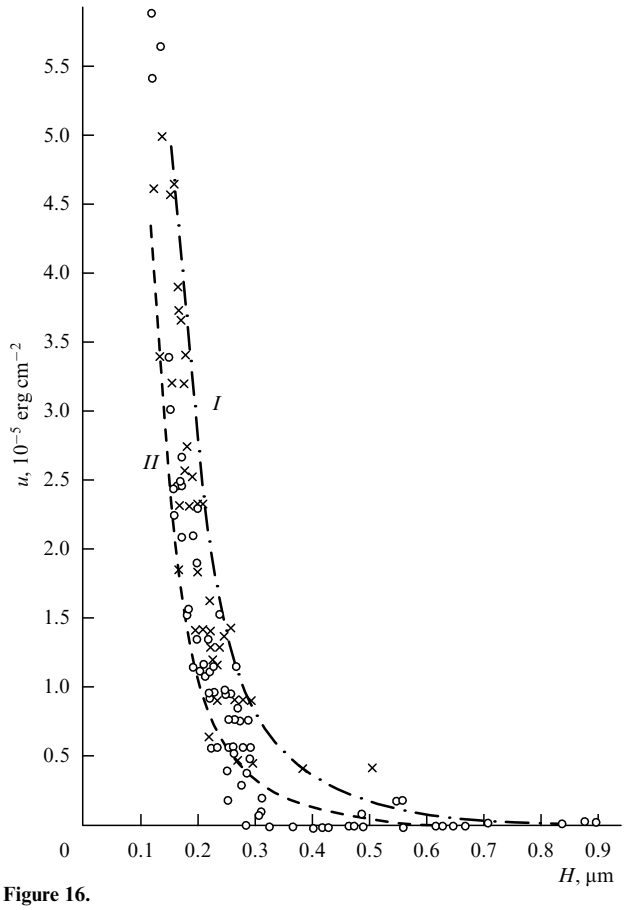

Figure 16.

6. Discussion

Since the results obtained relate to the discovery and measurement of an effect the existence of which has never before been demonstrated in direct experiments, we deem it opportune to analyze them in some detail and justify their interpretation.

6.1 Analysis of measurement data

The agreement between the results of measurements in air and in vacuum indicates that they do not depend on convection flows, the radiometer effect, the presence of a viscous air layer between bodies, or water vapor in the air.

Appropriate steps were taken to avoid measurement errors due to any unrecognized mechanical action of any part of the apparatus, e.g., elasticity of the electric wires carrying current to the frame, friction between the knife edge of the prism and the block, or dust particles remaining on the surface of the study bodies, and so forth. The elasticity of the wires was minimized by choosing very thin annealed Wollaston wires. The agate prism and block met all the requirements for such parts in the best microanalytical balances. In high quality balances with a beam and pan weight of a few dozen grams, the friction does not prevent weighing with a sensitivity down to $10^{-5}-10^{-6}$ g. Friction is known to be approximately proportional to the load. It is therefore clear why, in a balance with the beam weighing 0.1 g, friction between the prism and the block [14] was entirely negligible when measuring to within 10^{-7} g.

[14] If this friction could affect the measurements, it would alter the zero-point of the balance, i.e., current i_0, which in fact was never observed.

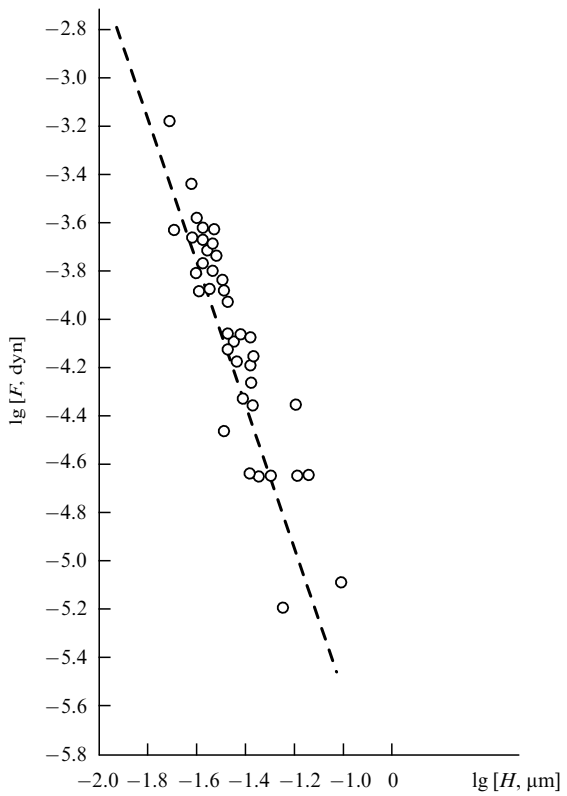

Figure 17.

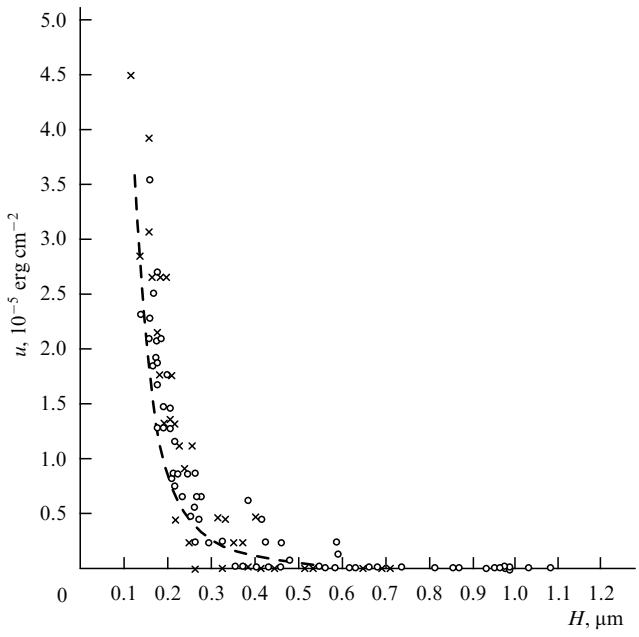

Figure 18.

The presence of dust particles on the body surfaces possibly affecting the measurements was always shown by the emergence of repulsive forces as the gap decreased; these were recorded by our apparatus with the same sensitivity as the attractive forces and never varied smoothly with the distance. Measurements were made only when no forces other than attractive were observed as the gap was reduced to 0.05–0.1 μm.

It is also certain that the observed attraction of bodies cannot be attributed to some film remaining on the surfaces after their cleaning. The presence of adsorbed water films on quartz surfaces is unavoidable in any measurements taken in air or in a low vacuum, and did not influence their results because, first, the distance between the bodies was much greater than the thickness of such films, and, second, the permittivity closely related to the strength of molecular attraction was about the same for the adsorbed films and the quartz. If film and quartz permittivities have a similar order of magnitude, the presence, for instance, of a 10-Å thick adsorbed film is equivalent to a change of the same order of magnitude in the gap width between the quartz surfaces, i.e., by 10 Å, which could not affect the results at the accuracy of the measurement of $H \sim 100$ Å.

In various experiments, different methods of surface cleaning were used. The curve in Fig. 11, for example, relates to experiments in which dust particles were removed with a degreased brush; those in Fig. 12 and others relate to the employment of ether and degreased cotton wool. If we assume that the attraction is caused by films of other substances, then the agreement between the results of numerous experiments would imply that in every case a film of the same type is present, which is too unlikely.

Even without a calculation, it is evident that the attractive forces shown, for example, in Fig. 12 have not a gravitational nature, since these cannot exhibit so strong a dependence on the gap width. As to the interaction forces between bodies due to electrization, they have been discussed in detail in the foregoing text.

6.2 Comparison with theory

Comparison with the calculation by summation over interactions between all pairs of molecules. If we choose to follow the method accepted until recently of summing the interactions between all pairs of molecules, formula (5′) is to be applied for the case of a sphere and a plane.

Substituting the experimental results into expression (5′), we find 5×10^{-14} erg for constant A. The constant A for quartz, however, is about 10^{-12} erg or 20 times the experimental value. This comparison illustrates that the calculation methods used hitherto are unsuitable, at least for distances on the order of 10^{-5} cm. We can therefore say that the experimental results have quite general significance, despite the limited number of objects measured.

With the same method of summation, but using Casimir's and Polder's correction, formula (7) is to be used for the energy.

Substituting our experimental results into expression (7), we find roughly 3×10^{-18} erg cm for constant A_1. The calculation from formula $A_1 = \pi^2 q^2 c_1$ gives $A_1 = 1 \times 10^{-18}$ erg cm. Polarizabilities α were taken from Margenau's review [12]. Here again, then, there is disagreement between experiment and theory, but much less than when the London interactions are summed.

Comparison with the macroscopic theory of molecular attraction. A precise comparison with Lifshitz's theory requires fairly complete knowledge of the optical properties of a material over its absorption regions without which the function $\varepsilon(\mathrm{i}\xi)$ cannot be constructed; however, the character of light absorption in quartz allows an approximate theoretical estimate.

In order to compare the theoretical results with directly measured quantities, some algebra is necessary. Integration

of expression (16) for $f(H)$ yields the attraction energy per unit area of two plates in the form

$$u(H) = -\frac{\hbar c}{3H^3}\frac{\pi^2}{240}\left(\frac{\varepsilon_0 - 1}{\varepsilon_0 + 1}\right)^2 \varphi(\varepsilon_0)\,. \tag{29}$$

The dashed curve in Fig. 14 depicts the $u(H)$ dependence as found from this formula, with ε_0 taken as the square of the refractive index of quartz glass in the optical range (see Section 3). To go from this energy to the interaction force between a sphere with radius R and a plane, we use the above relation, namely

$$F(H) = 2\pi R u(H)\,.$$

The dotted line in Fig. 13 shows the calculated dependence $F(H)$ for quartz samples. The dotted curves in Figs 15 and 16 present calculated results for thallium halides. Curves *I* correspond to the statical values of permittivity ε for a mixed crystal of thallium halides, and curves *II* to $\varepsilon = n^2 \approx 6$. (Here, as in quartz, the latter case may be regarded as more accurate.)

Figures 17 and 18 present in a similar way the dependence calculated for the chromium–quartz case. The Lifshitz theory gives, for the estimation of metal–dielectric interaction at large enough gaps, the following formula

$$f = \frac{\hbar c}{H^4}\frac{\pi^2}{240}\frac{\varepsilon_0 - 1}{\varepsilon_0 + 1}\varphi_1(\varepsilon_0)\,, \tag{30}$$

where $\varphi_1(\varepsilon_0)$ is the function tabulated in paper [24], and other notations are as in formula (16). Taking into account, as above, the transparency of quartz at wavelengths coincident with H, we used in the calculation the ε_0 value equal to the square of the refractive index of quartz in the optical range. Bearing in mind the approximate character of these theoretical predictions and the errors of measurement, the agreement found can be considered entirely satisfactory.

The agreement between experiment and theory as demonstrated in Figs 13–18 is to be regarded, on the one hand, as a confirmation of Lifshitz's theory and, on the other, as a significant proof of the molecular nature of the measured attraction between bodies.

The agreement of the experimental results with a theory which accounts for the molecular interaction as being occurred between electromagnetic fields present in any absorbing medium and extending outside gives the answer to the question posed by Lebedew away back in 1894 (see Introduction) [11, 12]. The molecular attraction indeed "reduces to electromagnetic forces" and does not involve "other forces of yet unknown origin."

Simultaneously with the present study, that of the Dutch scientists Overbeek and Sparnaay [37], who obtained altogether different results appeared. They measured the attractive forces between two plates of fused quartz with a dynamometer in which the spring strain was measured with an electric capacitive method; the distance between the parallel plates was found from the interference colors in the gap between them. To eliminate the influence of the air layer, the vacuum was maintained at 10^{-3} mmHg. This work was presented together with our own at a Faraday Society discussion in 1954 [38]. The Dutch authors' results were given as a logarithmic graph of the force dependence on distance and a calculation, assuming the validity of equation (6′), of the experimental value of constant A, which gave an obviously overestimated result of 3.8×10^{-11} erg. If the calculation is based on Lifshitz's theory with a spacing of 1200 Å between the quartz plates, the attractive force is found to be about 2×10^{-4} dyn cm^{-2}, whereas in Overbeek's and Sparnaay's experiments this distance corresponded to a force of 1 dyn cm^{-2}. The observed results therefore exceed the theoretical ones by a factor of almost 10^4. The poor reproducibility of Overbeek's and Sparnaay's results and the too high a magnitude of the attraction effect found in their experiments seem to have been due to charging of the surface.

In recent work by Prosser and Kitchener [39, 40], the molecular attraction between glasses was measured by a method[15] similar to that of Overbeek and Sparnaay, but their results agree with ours and with the Lifshitz theory.

6.3 Applications to coagulation theory

According to Fuchs's theory [41], the rate of coagulation of a disperse system whose particles with radius r attract one another with an energy $u(x)$ depending on the distance x between their centers increases relative to the case of $u(x) = 0$ discussed by Smoluchowski by a factor of

$$1 : 2r\int_{2r}^{\infty}\frac{\exp\left[-u(x)/kT\right]\,\mathrm{d}x}{x^2} = 1 : \int_0^{\infty}\frac{\exp\left[-u(\tau)/kT\right]\mathrm{d}\tau}{(1+\tau)^2}\,, \tag{31}$$

where

$$\tau = \frac{x - 2r}{2r}\,.$$

If r is sufficiently small (in comparison with the wavelengths of the principal bands in the absorption spectrum of the particles), then for values satisfying the condition

$$x - 2r \ll 2r\,,$$

u can be expressed as follows:

$$u = \frac{A\,2r}{24(x - 2r)} = \frac{1}{24}\frac{A}{\tau}\,.$$

Taking into account that $A/24$ and kT are quantities of the same order, the coefficient of coagulation acceleration rate is much higher than unity,[16] because u/kT is large enough within a wide range of τ values starting from 0. In this case, the acceleration coefficient will be independent of r. However, the result is different if r is sufficiently large. Indeed, for sufficiently large r, the main part of the integral in formula (31) corresponds to x values for which a correction for electromagnetic retardation needs to be introduced for reducing u and therefore the acceleration of coagulation. This accounts for the very low acceleration of coagulation under the effect of molecular forces, for example, in aerosols with particles having $r > 0.2$ μm.

The situation is different for the coagulation of lyophobic sols, where not only the attraction energy but also the

[15] Because of the high sensitivity of the appropriate apparatus to vibrations, measurements could be made only at night. Also, it was necessary to control thermostatically not only the apparatus itself but the entire laboratory in order to reduce zero-creep. Finally, a high vacuum was needed. This confirms the advantages of our above-discussed feedback-assisted method.

[16] This conclusion was reached previously in paper [43].

repulsion energy, when the ionic atmospheres of two particles overlap, are important. Here, when the particles are sufficiently large, the two interaction energy terms (at distances at which they are appreciable) are proportional to the radius; hence, the presence or absence of an energy barrier for the resultant interaction on which the stability of the system actually depends according to the theory developed previously [2–8] is independent of the radius. According to the same theory, the stability of the system with respect to coagulation depends on the behavior of the attractive forces at distances on the order of the thickness of ionic atmospheres. It is therefore evident that when the latter is small (below 10^{-6} cm), i.e., for medium and high electrolyte concentrations, only the behavior of the molecular forces at distances that do not need corrections for electromagnetic retardation is important. Therefore, the previously developed theory of stability of sols [2–8] remains valid; in particular, the coagulating action is proportional to the sixth power of the counter-ion charge for highly charged colloidal particles (the Hardy–Schulze law).

The border of validity of this law is accordingly not related to the radius of the particles [17] but to the concentration: at very low concentrations, taking account of the faster (by one power of the gap width) decrease of the attractive forces at large distances, it is easy to show for highly charged sols that the sixth power must be replaced by the eighth power. Since very small coagulating concentrations can be observed here only for counter-ions with high charges (trivalent and tetravalent), it follows that only in such cases is the relevant effect to be expected.

In the opposite limiting case of sol coagulation due to a charge decrease, a low concentration can be observed at any ion charge. The law of inverse proportionality between the critical potential corresponding to the threshold of coagulation and the square root of the ion atmosphere thickness, valid for moderate electrolyte concentrations, must then go over to the one between the potential and the ion atmosphere thickness itself, which can be verified experimentally.

6.4 Applications to wetting theory

The measured values of heat or energy of wetting are often used in comparisons with the formulas for dispersive forces. This, however, leads to two errors, the influence of which is certainly great even if difficult to assess precisely: (1) the molecular forces are assumed to be additive, and (2) the main contribution to the heat of wetting comes from the interaction between molecules of the wetted surface and the wetting liquid in direct contact. Meanwhile, it is precisely for molecules which are near-neighbors that London's formulas are essentially invalid.

The situation is different for the wetting of an originally dry body or its parts. The kinetics and even the qualitative result of such effects may be independent of the interactions at short distances, being determined mainly by the molecular interaction at distances many times the molecular diameters.

Let us consider the specific case of a broad strip moving round two shafts and coming at point A into contact with liquid in a vessel. It was shown in an experiment that, as the velocity U of the strip increases, the wetting angle α, even if initially zero, increases, tending toward $\alpha = 180°$. At the same time, the wetting line, the projection of which is point A in

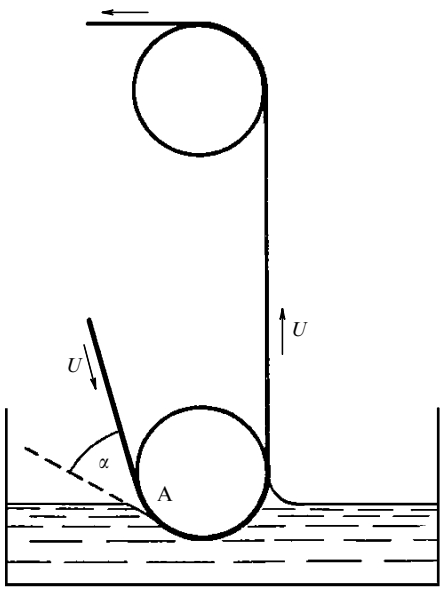

Figure 19.

Fig. 19, will move to the right and there can no longer be 'perfect' contact with the liquid for $U > U_c$.[18] The velocity U_c can be calculated if the length L is assumed to be so great that U_c will virtually correspond to the displacement of point A to infinity.

Using methods of capillary hydrodynamics and knowing the dependence of the molecular attraction on the gap width, one can find U_c. When the angle β at which the strip enters the liquid is small, the most important forces are those acting at relatively short distances H, when the simpler limiting case of interaction with electromagnetic retardation occurs in accordance with the law $f = A_1 H^{-4}$. This gives the formula

$$U_c = C(1 - \cos\beta)^{9/16} \frac{A_1^{3/8} \sigma^{1/16} (\rho g)^{9/16}}{\eta} ,$$

where η is the viscosity of the liquid, σ is its surface tension, ρ is its density, g is the acceleration of gravity, β is the angle between the strip and the horizontal plane, and C is a constant that can be calculated by numerical integration of a nonlinear second-order differential equation with constant coefficients.

Having this formula, and knowing U_c from experiments, one can calculate constant A_1. In measuring U_c, it is, of course, necessary to be sure of eliminating electrostatic effects, which is more complicated in this case. On the other hand, here there is neither the harmful effect of dust particles or vibrations nor any need to measure weak forces and small gaps.

References

1. Kallmann H, Willstätter M *Naturwissenschaften* **20** 952 (1932)
2. Derjaguin B V *Kolloid. Zh.* **6** 291 (1940)
3. Derjaguin B V *Kolloid. Zh.* **7** 285 (1941)
4. Derjaguin B V *Trans. Faraday Soc.* **36** 203 (1940)
5. Derjaguin B V *Trans. Faraday Soc.* **36** 730 (1940)
6. Derjaguin B, Landau L *Acta Physicochim. URSS* **14** 633 (1941)

[17] Thus, one cannot agree with Overbeek's assertion that for large particles the law requires correction for electromagnetic retardation.

[18] There can, however, be imperfect contact over several areas separated by unwetted ones, because of the instability of the liquid surface in the molecular attraction field of the strip surface.

7. Derjaguin B V, Landau L D *Zh. Eksp. Teor. Fiz.* **11** 802 (1941)
8. Derjaguin B V, Landau L D *Zh. Eksp. Teor. Fiz.* **15** 662 (1945)
9. Verwey E J W, Overbeek J Th G *Theory of the Stability of Lyophobic Colloids* (New York: Elsevier Publ. Co., 1948)
10. Langmuir I *J. Chem. Phys.* **6** 873 (1938)
11. Lebedev P N *Sobranie Sochinenii* (Collected Papers) (Moscow: Mosk Fiz. Obshch. im. P N Lebedeva, 1913) pp. 56–57
12. Lebedew P *Wied. Ann.* **52** 621 (1894)
13. Galitzin B *Izv. Imperator. Akad. Nauk* **3** (1) 1 (1895); *Bull. Acad. Impériale Sci. St.-Pétersbourg* **3** (1) 1 (1895)
14. London F *Z. Phys.* **63** 245 (1930)
15. Bradley R S *Phil. Mag.* **13** 853 (1932)
16. London F *Z. Phys. Chem.* **11** 222 (1931)
17. Casimir H B G, Polder D *Phys. Rev.* **73** 360 (1948)
18. London F *Trans. Faraday Soc.* **33** 8 (1937); *Usp. Fiz. Nauk* **17** 421 (1937)
19. Margenau H *Rev. Mod. Phys.* **11** 1 (1939)
20. de Boer Y H *Trans. Faraday Soc.* **32** 10 (1936)
21. Hamaker H C *Physica* **4** 1058 (1937)
22. Rytov S M *Theory of Electric Fluctuations and Thermal Radiation* (Bedford, Mass.: Electronics Research Directorate, Air Force Cambridge Research Center, Air Research and Development Command, U. S. Air Force, 1959); Translated from Russian: *Teoriya Elektricheskikh Fluktuatsii i Teplovogo Izlucheniya* (Moscow: Izd. AN SSSR, 1953)
23. Landau L D, Lifshitz E M *Electrodynamics of Continuous Media* (Oxford: Pergamon Press, 1984); *Elektrodinamika Sploshnykh Sred* (Moscow: Gostekhizdat, 1957)
24. Lifshitz E M *Sov. Phys. JETP* **2** 73 (1956); *Zh. Eksp. Teor Fiz.* **29** 94 (1955)
25. Casimir H B G *Proc. Kgl. Ned. Akad. Wet.* **60** 793 (1948)
26. Derjaguin B V *Dokl. Akad. Nauk SSSR* **61** 275 (1948)
27. Derjaguin B V, Abrikosova I I *Dokl. Akad. Nauk SSSR* **90** 1055 (1953)
28. Derjaguin B V, Abrikosova I I *Dokl. Akad. Nauk SSSR* **108** 214 (1956)
29. Derjaguin B V, Abrikosova I I *Zh. Eksp. Teor. Fiz.* **21** 945 (1951)
30. Deryagin B V, Abrikosova I I *Sov. Phys. JETP* **3** 819 (1957); *Zh. Eksp. Teor. Fiz.* **30** 993 (1956)
31. Deryagin B V, Abrikosova I I *Sov. Phys. JETP* **4** 2 (1957); *Zh. Eksp. Teor. Fiz.* **31** 3 (1956)
32. Deryagin B V, Abrikosova I I *Sov. Phys. JETP* **6** 615 (1958); *Zh. Eksp. Teor. Fiz.* **33** 799 (1957)
33. Derjaguin B V, Abrikosova I I, Lifshitz E M *Q. Rev. Chem. Soc.* **10** 295 (1956)
34. Derjaguin B V, Titijevskaia A S, Abricossova I I, Malkina A D *Discuss. Faraday Soc.* **18** 24 (1954)
35. Derjaguin B V *Zh. Fiz. Khim.* **6** 1306 (1935)
36. Kurbatov L N *Zh. Fiz. Khim.* **28** 287 (1954)
37. Overbeek J Th G, Sparnaay M J *J. Colloid. Sci.* **7** 343 (1952)
38. Overbeek J Th G, Sparnaay M J *Discuss. Faraday Soc.* **18** 12 (1954)
39. Prosser A P, Kitchener J A *Nature* **178** 1339 (1956)
40. Kitchener J A, Prosser A P *Proc. R. Soc. Lond. A* **242** 403 (1957)
41. Fuchs N *Z. Phys.* **89** 736 (1934)
42. Petryanov I V, Tunitskii N N *Zh. Fiz. Khim.* **17** 408 (1943)
43. Petryanov I V, Tunitskii N N *Acta Physicochim. URSS* **18** 185 (1942)